IAG GEOMORPHOLOGY GEOMORPHOLOGIE AIG

11TH IAG INTERNATIONAL CONFERENCE ON GEOMORPHOLOGY

FIELDTRIP GUIDE

SEISMICALLY INDUCED LANDSCAPE EVOLUTION AND ENVIRONMENTAL IMPACTS IN ŌTAUTAHI CHRISTCHURCH

2026

11TH IAG INTERNATIONAL CONFERENCE ON GEOMORPHOLOGY

2–6 February 2026

Christchurch, New Zealand (Ōtautahi, Aotearoa)

COMPILED FOR THE 11TH IAG INTERNATIONAL CONFERENCE ON GEOMORPHOLOGY

ŌTAUTAHI, AOTEAROA
CHRISTCHURCH, NEW ZEALAND
2026

Cover Photos: Wairongomai-Mangarara (Credit: Ian Fuller), Aoraki Mt. Cook National Park (Credit: Sam McColl), and Waikato at Taupo (Credit: Sarah McSweeney).

Seismically-Induced Landscape Evolution and Environmental Impacts in Ōtautahi Christchurch

Date: Wednesday 4 February

Departs from: Christchurch

Ends: Christchurch

Leaders: Mark Quigley (University of Melbourne), Brendan Duffy (GHD), Catherine Reid (University of Canterbury), Sarah Barrett (BECA)

Brief Description

The fieldtrip will take participants to selected sites in eastern Christchurch and in the Port Hills that experienced geomorphic change resulting from the 2010-2011 Canterbury earthquake sequence (CES). We will first visit Rapaki in the Port Hills (Stop 1), where hundreds of rockfalls occurred during the CES, and where evidence for pre-CES (paleo-) rockfalls was investigated. We will then travel to Sumner (Stop 2), where extensive cliff collapse occurred. A visit to a tidally-dominated estuary site in eastern Christchurch (Stop 3) will examine geomorphic and biological responses to uplift and subsidence associated with fault displacements and liquefaction settlement. We will finish in the residential red zone in the suburb of Avonside (Stops 4,5), where numerous geological-geomorphic-geotechnical studies were undertaken in the aftermath of the CES and where upwards of 0.5m of surface subsidence occurred.

Start and finish locations: The trip begins and ends at Te Pae.

Start and finish times: Commences at 9.00 am, Finishes at 4.00 pm.

What to bring:

- Water
- Snacks and Lunch
- Sun protection (sunhat, sunscreen)
- Warm clothing
- Water/windproof jacket
- Hiking shoes
- Personal medication

What to expect: Short walks on flat and sloping ground, including some small hillwalking. Maximum distance walked at any site will be about 300 m.

Cite this guide as:

Quigley, M., Duffy, B., Reid, C., Barrett, S. (2026) Seismically-Induced Landscape Evolution and Environmental Impacts in Ōtautahi Christchurch: Mid-Conference Field-trip Guide; 11th IAG International Conference on Geomorphology, Christchurch Otautahi, New Zealand Aotearoa, 4 February, 43 p.


Stop 5
Stop 4
Stop 3
The Bridge South Brighton Trust
South New Brighton
Sumner Stop 2
Rapaki boulders STOP 1

STOP 1: Rāpaki rockfall site (Te Rāpaki-o-Te Rakiwhakaputa), Banks Peninsula / Port Hills, Christchurch *(Mark Quigley)*

STOP 1: Rāpaki rockfall site (Te Rāpaki-o-Te Rakiwhakaputa), Banks Peninsula / Port Hills, Christchurch *(Mark Quigley)*

1) Purpose and learning outcomes

This trip examines an internationally well-studied earthquake-induced rockfall "natural laboratory" on the eastern flanks of Te Poho o Tamatea (Mount Rapaki), where hundreds of boulders were mobilised during major events of the 2010–2011 Canterbury earthquake sequence (CES), including the 22 February and 13 June 2011 earthquakes. nhess.copernicus.org+1
By the end of the trip, participants should be able to:

- Identify the dominant source lithologies (volcanic breccia vs coherent lava basalt) and structural controls on detachment and block shape. nhess.copernicus.org
- Distinguish "contemporary" CES boulder populations from older (prehistoric) boulders using geomorphic and weathering indicators (e.g., lichen cover, surface roughness, partial burial/exhumation). drquigs.com+1
- Explain why modern boulders at Rāpaki can show longer runout distances than prehistoric counterparts, and how land-cover change (deforestation) modifies trajectory, energy loss, and stopping mechanisms. Science+1
- Connect site observations to post-earthquake risk assessment and land-use decisions in the Port Hills (hazard, exposure, vulnerability, and risk tolerability). Christchurch City Council+1

---

2) Cultural context and fieldwork protocol

Rāpaki is a long-occupied settlement and marae-based community of Te Hapū o Ngāti Wheke (Ngāi Tahu), within Whakaraupō / Lyttelton Harbour. Te Poho o Tamatea is a culturally significant maunga. ngaitahu.iwi.nz+1
Field protocol expectations:

- Treat the area as a lived cultural landscape, not just a geomorphic site.
- Stay on public tracks/road verges unless you have explicit permission for access. Bus will be parked on north side of Governors Bay Rd.
- Minimise disturbance: no sampling, digging, or boulder/soil excavation without permissions and an agreed research plan.

---

3) Safety and risk management (non-negotiable)

Rockfall terrain is inherently hazardous, and risk can be elevated after strong ground shaking and intense rainfall.

- **Do not enter active fall lines** beneath cliffs or overhangs; avoid lingering below steep source faces.
- Grass fire is a risk at this time of year – please do not use any ignition sources.
- Long grass may obscure your view of foot placement – please take care
- Maintain **wide spacing** when moving through boulder fields; use **spotters** when traversing steep grassed slopes.
- Wear sturdy boots; helmets are recommended if approaching talus or source cliffs.

- Weather: Port Hills winds and rapid cloud changes are common; carry layers and water.
- Refer to Christchurch City Council Port Hills slope-stability information and mapped rockfall/cliff-collapse hazard context for planning and exclusions. Christchurch City Council+1

Stop 1A — Rāpaki village / toe-slope viewpoint: "From hazard process to consequences"

Theme: Linking hillslope process to exposure and impacts.
What to observe

- Overall hillslope geometry: concave-to-planar slope feeding into the settlement footprint. nhess.copernicus.org+1
- Evidence of boulder emplacement and runout pathways that can reach developed areas during strong shaking (documented during CES). nhess.copernicus.org+1

Discussion prompts

- What aspects of exposure and vulnerability (housing placement, road corridors, occupancy patterns) matter most here?
- How do agencies translate mapped hazard into zoning, managed retreat, or engineered protection?

Stop 1B — Lower–mid slope boulder field: "Modern vs prehistoric rockfall signatures"

Theme: Reading the boulder record as an event archive.
What to observe

- Coexisting boulder populations: CES boulders vs older boulders with stronger weathering/lichen signals and partial burial/exhumation histories. drquigs.com+1
- Boulder interaction effects: older boulders and drainage-line boulder concentrations can deflect, slow, or stop later boulders. nhess.copernicus.org

Exercise (20–30 min)

- In small groups, select 6–10 boulders and record:
    - Apparent lithology (volcanic breccia vs coherent lava) and block morphology
    - Relative surface weathering/lichen presence (qualitative scale)
    - Slope position and whether the boulder sits in a drainage line
- Use observations to classify each boulder as "likely CES" vs "likely prehistoric," and justify.

Key interpretive takeaway
Borella and Quigley's work demonstrates that prehistoric boulders are abundant at Rāpaki and likely relate to prehistoric earthquake activity. Their distributions present a comparator population for understanding how recent events behave differently. Science+1

Stop 1C — Mid-slope process station: "Why do some modern boulders travel farther?"

Theme: Runout physics meets land-cover change.
What to observe

- Surface roughness contrasts, grass cover, and the relative absence of dense native forest on many slopes.
- Evidence that land-surface conditions and vegetation strongly modulate energy dissipation and stopping distances.

Teaching notes
A central conclusion from Borella, Quigley and colleagues is that some modern (Anthropocene) boulders at Rāpaki exhibit longer runouts than prehistoric boulders, consistent with reduced forest "braking" and altered hillslope surface conditions following deforestation. Science+1

- Compare boulders in open grassed slope vs drainage lines vs behind other boulders, and discuss why stopping mechanisms differ.

Stop 1D — View upslope to Upper slope / source-rock viewpoint: "Lithology, structure, and detachment"

Theme: Why blocks detach, and why they look the way they do.
What to observe

- Source cliffs near the top of Te Poho o Tamatea include steep to near-vertical exposures where CES detachments occurred, and where volcanic breccia (VB) and coherent lava (CL) layering and fracture patterns influence detachment frequency and block morphology. nhess.copernicus.org+1
- Conduct a rapid **structural scan** (visual, no climbing):
  - Dominant joint sets, spacing, and persistence
  - Block size expectations from joint spacing
  - Which lithology appears more prone to producing equant vs slabby blocks?
- Tie this back to mapped lithologic contrasts described in the Rapaki studies. nhess.copernicus.org

---

Synthesis viewpoint: "From palaeorockfall chronologies to future hazard"

Theme: What the late Holocene record implies—and what it does *not* imply.
What to cover

- Prehistoric rockfalls at Rāpaki have been dated and interpreted as evidence of strong local shaking events capable of producing large boulder falls, providing a longer-term perspective on recurrence and hazard plausibility. drquigs.com+1
- Critical nuance: a single-site palaeorockfall record constrains *site response and local triggering thresholds*, but does not directly yield a complete seismic hazard model for Canterbury without broader fault and shaking context. AGU Blogosphere

REFERENCES FOR STOP 1:

Borella, J. W., Quigley, M. C., & Vick, L. M. (2016). Anthropocene rockfalls travel farther than prehistoric predecessors. Science Advances, 2(9), e1600969. https://doi.org/10.1126/sciadv.1600969

Borella, J. W., Quigley, M. C., Bebbington, M., & Vick, L. M. (2019). Geologic and geomorphic controls on rockfall hazard: How well do past rockfalls predict future distributions? Natural Hazards and Earth System Sciences, 19(10), 2249–2280. https://doi.org/10.5194/nhess-19-2249-2019

Christchurch City Council. (n.d.). Mass movement in the Port Hills. https://ccc.govt.nz/environment/land/slope-stability/mass-movement-or-landslides

Christchurch City Council. (n.d.). Port Hills GNS reports. https://ccc.govt.nz/environment/land/slope-stability/porthillsgnsreports

GeoTrips (GNS Science). (n.d.). Rapaki Dyke. https://www.geotrips.org.nz/trip.html?id=718

Mackey, B. H., & Quigley, M. C. (2014). Strong proximal earthquakes revealed by cosmogenic 3He dating of prehistoric rockfalls, Christchurch, New Zealand. Geology, 42(11), 975–978. https://doi.org/10.1130/G36149.1

Ngāi Tahu. (n.d.). Rāpaki. https://ngaitahu.iwi.nz/ngai-tahu/papatipu-runanga/rapaki/

Quigley, M. C., Hughes, M. W., Bradley, B. A., van Ballegooy, S., Reid, C., Morgenroth, J., Horton, T., Duffy, B., & Pettinga, J. R. (2016). The 2010–2011 Canterbury Earthquake Sequence: Environmental effects, seismic triggering thresholds and geologic legacy. Tectonophysics, 672–673, 228–274. https://doi.org/10.1016/j.tecto.2016.01.044

Rāpaki Marae (Te Hapū o Ngāti Wheke). (n.d.). Kāinga: Home. https://rapaki.iwi.nz/

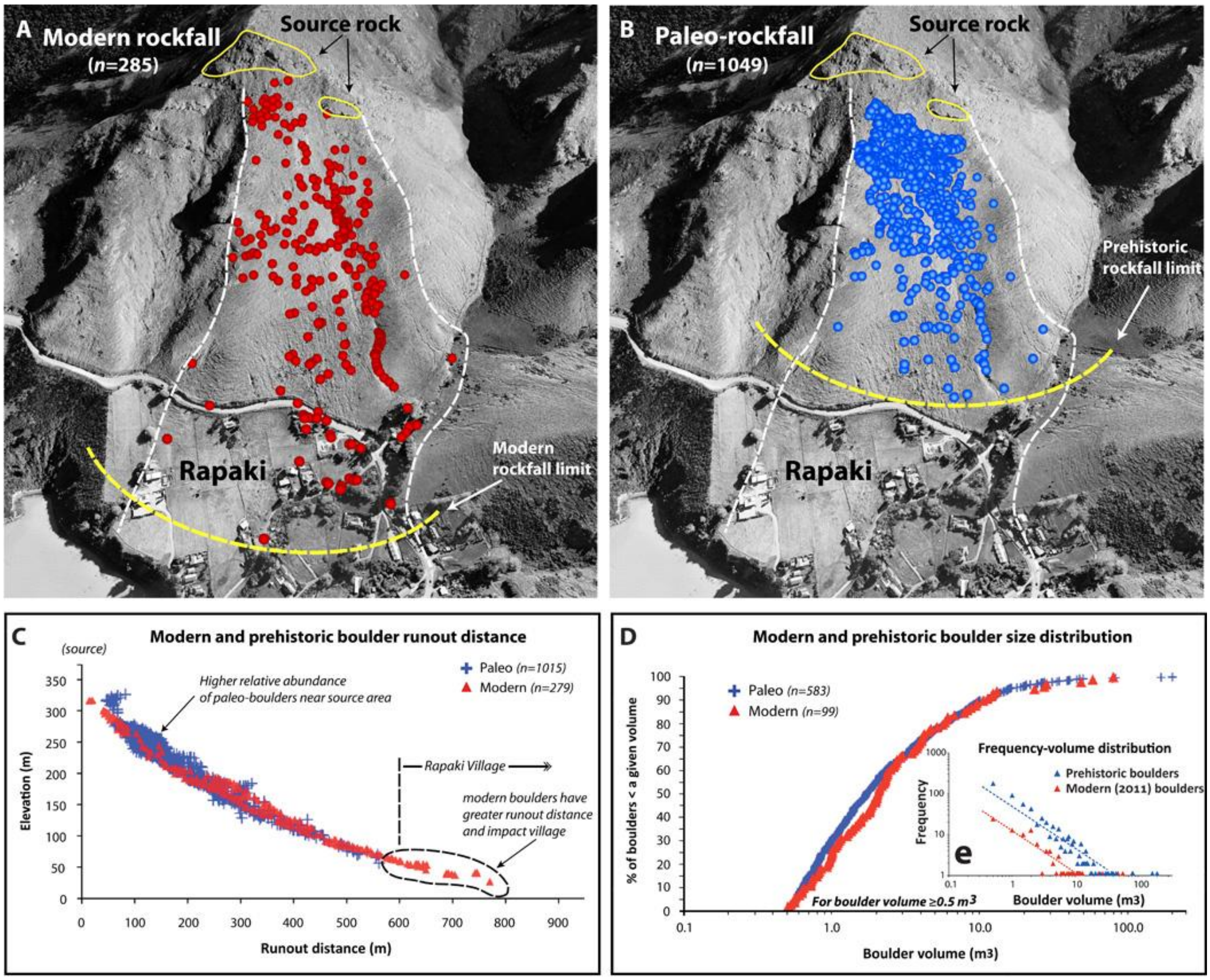

Spatial distribution and size comparison of modern and prehistoric rockfall at Rapaki.

(**A**) Spatial distribution for mapped modern rockfall (*n* = 285) generated during the 2011 Christchurch earthquakes (22 February and 13 June events). Twenty-six modern boulders affected the Rapaki village and caused severe damage to residential properties. Maximum runout distance (map length) for modern boulders is ~770 m. (**B**) Spatial distribution for mapped paleoboulders (*n* = 1049). No evidence for prehistoric boulders in area now occupied by the Rapaki village. Maximum travel distance for prehistoric boulders is ~560 m. (**C**) Modern and prehistoric rockfall runout distance plotted as function of elevation. Travel distance for modern rockfalls exceeds limit of prehistoric predecessors. (**D**) Comparison of boulder size distribution for modern and prehistoric boulders indicates strong similarity. (**E**) The frequency-volume distributions for prehistoric and modern rockfall at Rapaki show a similar power-law trend.

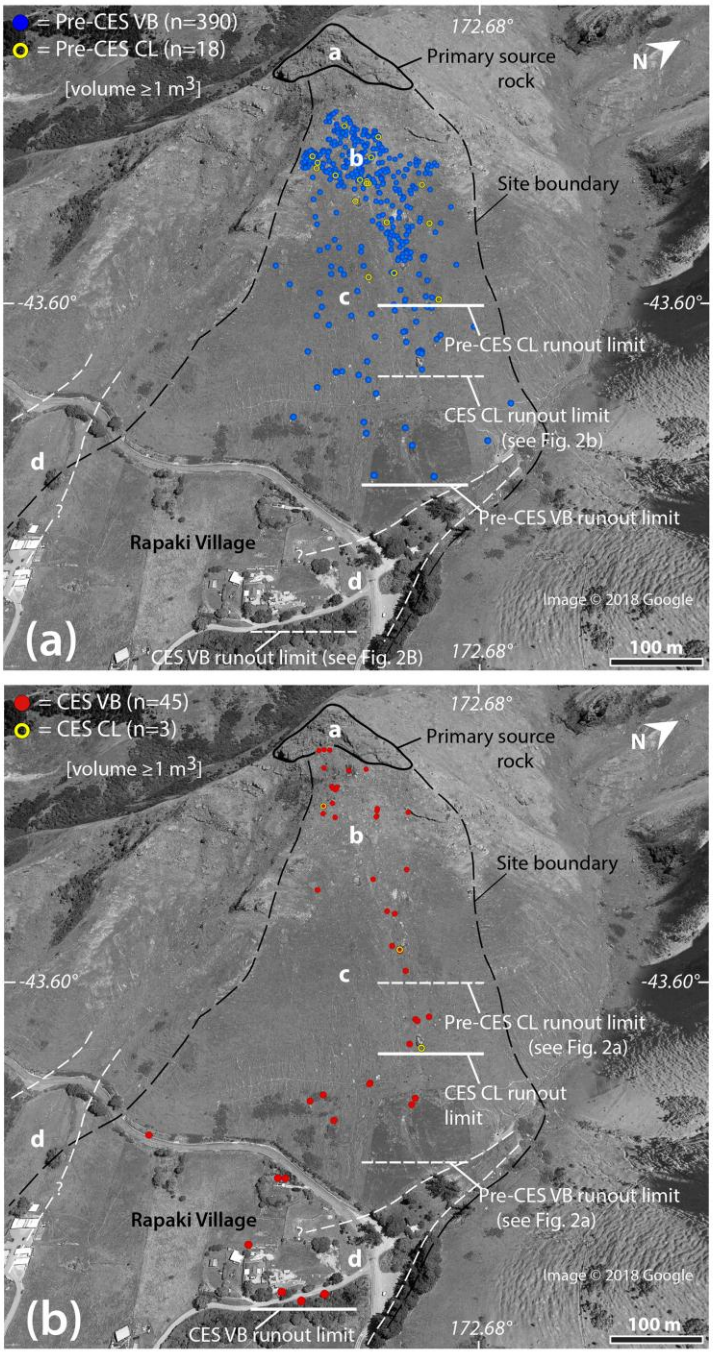

(a) Mapped pre-CES volcanic breccia (VB) and coherent lava (CL) boulders with volume ≥ 1.0 m^3 at Rapaki. The largest boulders with the furthest runout distances are comprised exclusively of volcanic breccia. Ratio of pre-CES VB to CL boulders is . **(b)** Mapped CES VB and CL boulders at Rapaki study site. Note the low number of CL rockfall boulders detached during the CES at Rapaki. Ratio of CES VB to CL boulders is 15:1 (a : volcanic source rock; b : dominated by volcanic boulder colluvium and volcanic loess colluvium; c : loess colluvium underlain by in situ loess and volcanic rock; d : alluvial sediments overlying loess and bedrock).

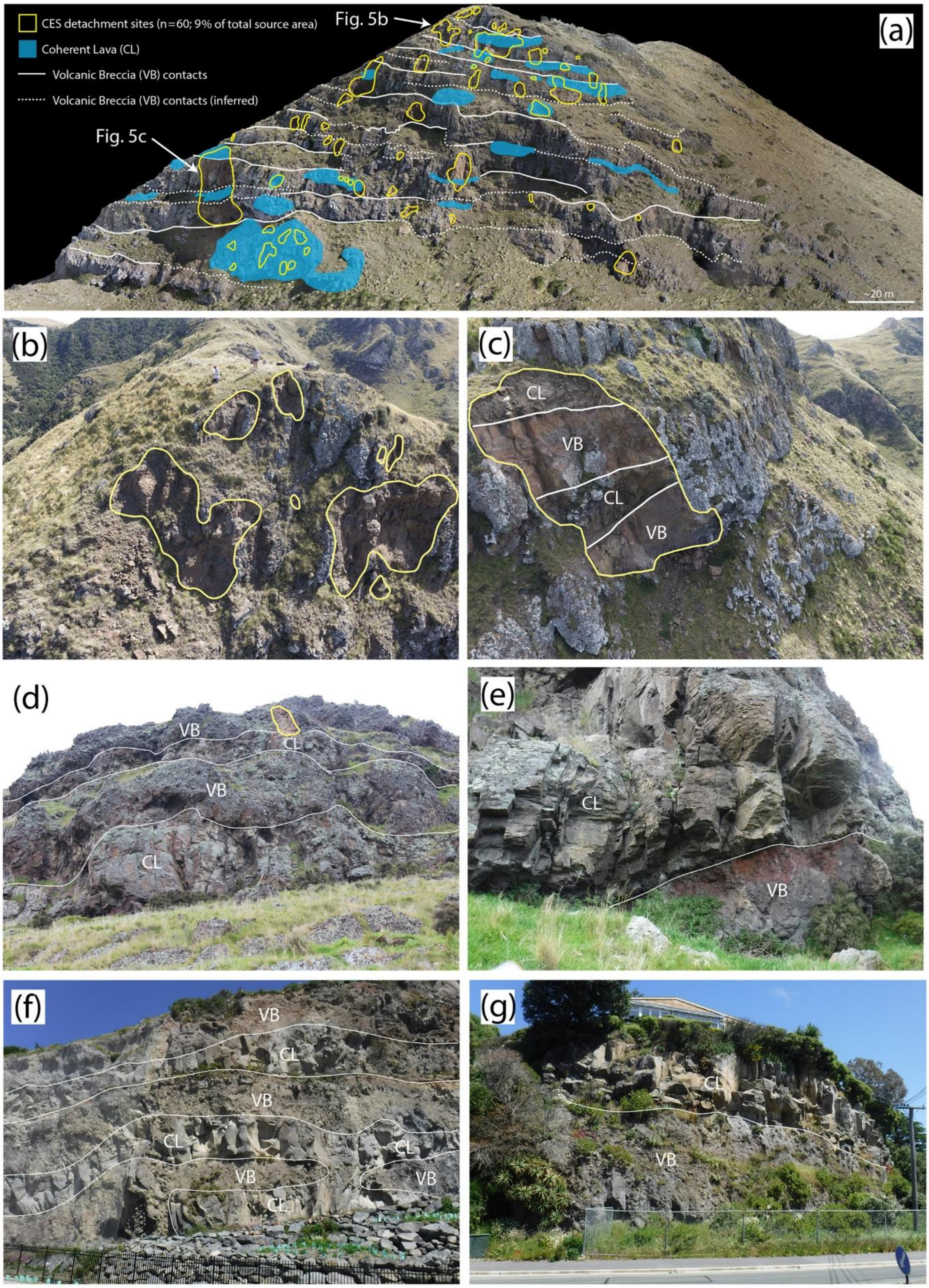

Figure 5(a) Volcanic source rock at Rapaki study site. Sixty individual detachment zones were created during the CES (yellow) and represent ~9 % of the total source rock area. The source rock is comprised of ~86 % VB and ~14 % CL. Approximately ~69 % and ~31 % of the detachments occurred within the VB and CL lithologies, respectively. **(b)** Photo showing several irregularly shaped CES detachment zones near the top of Mount Rapaki. **(c)** Photo showing freshly exposed VB and CL layering within the Rapaki source rock. **(d)** Portion of volcanic source rock at Purau showing VB and CL layering. A single CES detachment site is shown at the top of the source rock. Seven individual CES detachment sites were identified at the Purau study site. **(e)** CL and VB layers at the Purau study site. Note the thickness of the CL layer (~5–7 m) and lack of any CES detachment sites despite the high degree of fracturing and overhanging condition. **(f)** VB and CL layering in Sumner (Christchurch) cliff exposure adjacent to Main Road. Extensive cliff collapse during the CES has revealed multiple lava flows and the distinctive textural differences between the VB and CL lithologies. Note the high density of vertical to subvertical fractures within the CL layers. **(g)** Exposed lava layers adjacent to Main Road in Redcliffs (Christchurch). Note the single-family living residence at top of photo.

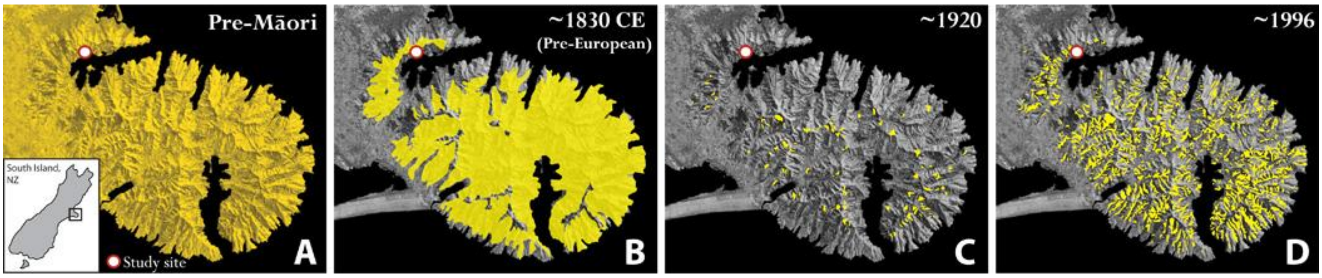

Anthropogenic deforestation of Banks Peninsula.

Removal of native forest (yellow) occurred rapidly in Banks Peninsula with the arrival of Polynesians (ca. 1280 CE) then Europeans (ca. 1830 CE). (**A**) Before arrival of the Polynesians (Māori), extensive native forest was present throughout Banks Peninsula. (**B**) Before European settlement, minor to moderate removal of indigenous forest by Māori had occurred in Banks Peninsula. Burning was the primary tool for clearance. (**C**) By 1920, Europeans had removed >98% of the native forest in Banks Peninsula, leaving slopes barren and low-lying areas vulnerable to slope hazards. (**D**) Minor reestablishment of old-growth native forest has occurred, but slopes in Banks Peninsula and the Port Hills (including Rapaki) remain largely unvegetated [data from previous studies

Modern boulder at Rapaki study site.

Photo of large modern boulder (~28 m^3) detached from Mount Rapaki and emplaced in the Rapaki village during the 22 February 2011 earthquake (photo courtesy of D. J. A. Barrell, GNS Science). The boulder traveled through the center of the residential home located in background (center). Boulder runout distance from source was ~700 m. Runout distance for furthest traveled modern boulders is significantly greater (~150 to 175 m) than travel distance for prehistoric boulders.

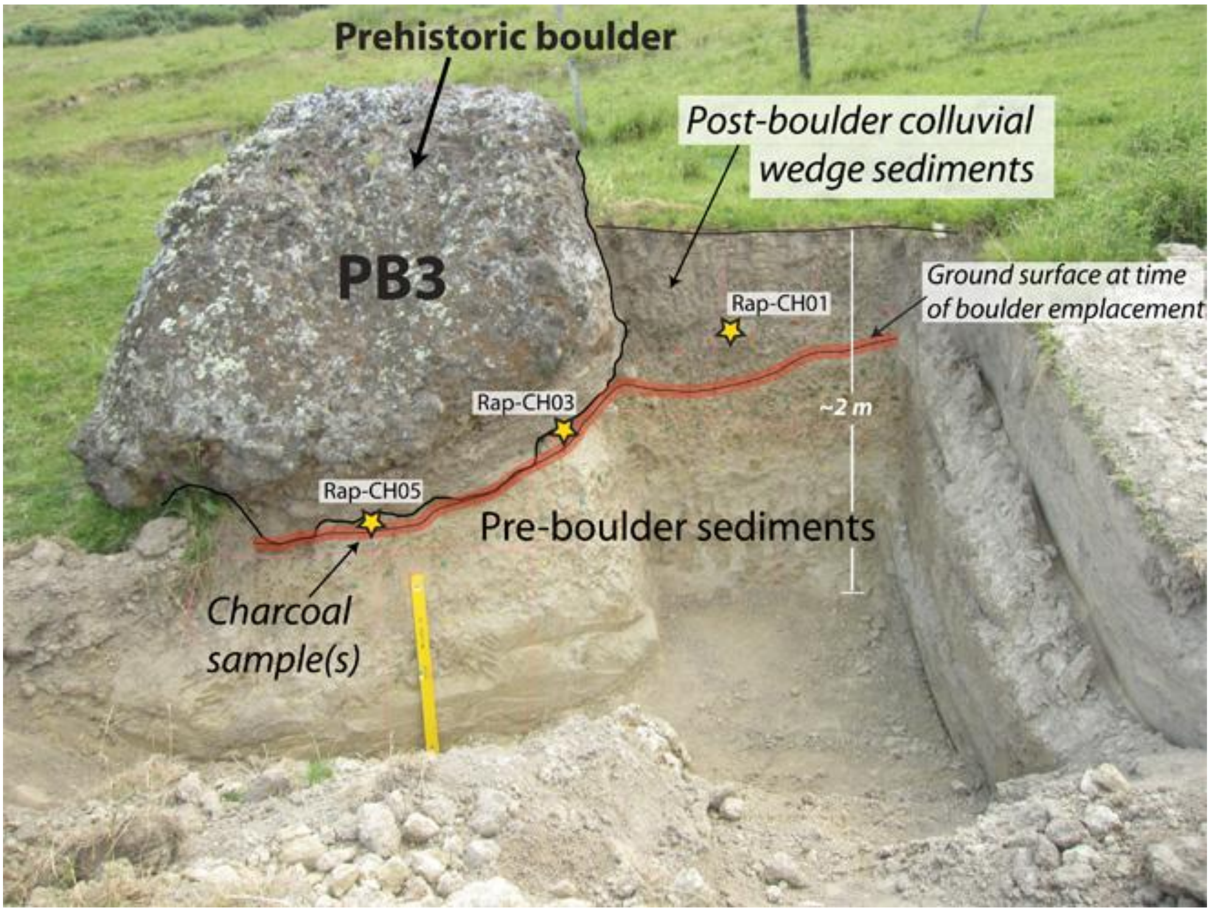

Prehistoric boulder at Rapaki study site.

Photo of exploratory trench excavated adjacent to Paleo-Boulder 3 (PB3), exposing hillslope sediments deposited before and after boulder emplacement. Locations for charcoal samples (yellow) Rap-CH01, Rap-CH03, and Rap-CH05 are shown. All samples were collected near the base of the most recent loess colluvial wedge sediments and yield similar conventional radiocarbon ages (203 ± 18, 197 ± 17, 222 ± 17 yr B.P., respectively). 2σ-Calibrated ages suggest a probable burning event occurred at Rapaki sometime between 1661 CE and 1950 CE, with highest 2σ subinterval probability between 1722 CE and 1810 CE. PB3 is deposited in footslope position, and volume is ~14.5 m^3. Total travel distance for PB3 is ~560 m.

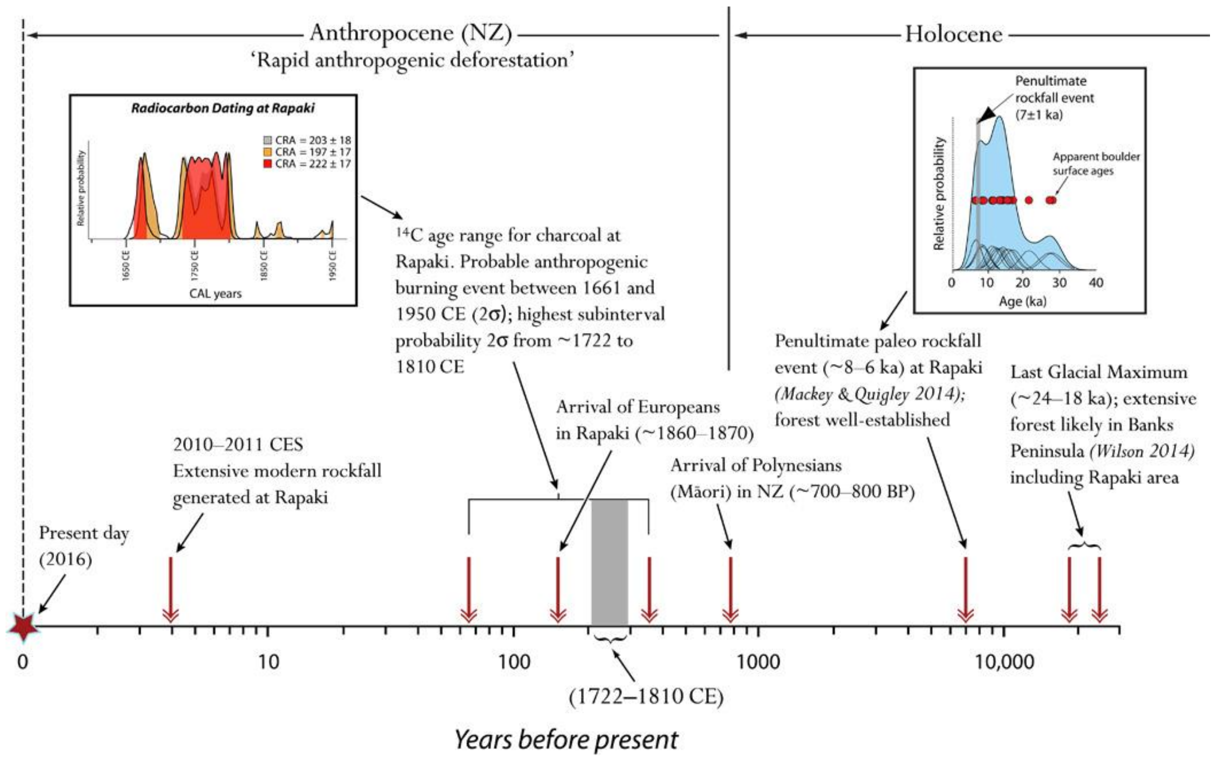

Rockfall and Anthropocene chronology for Rapaki study site.

Native forest likely persisted during the Last Glacial Maximum and thrived during the Holocene in Banks Peninsula and at Rapaki. The penultimate paleorockfall event at Rapaki occurred approximately 8 to 6 ka [taken from the study of Mackey and Quigley (23)] when a dense variable forest cover would have existed on the hillslope. Radiocarbon dating of charcoal at Rapaki suggests a probable burning event occurred sometime between 1661 CE and 1950 CE, with highest subinterval probability between 1722 CE and 1810 CE. Slope deforestation by Māori and later Europeans allowed modern rockfall generated during the 2011 Christchurch earthquakes to travel further than their prehistoric predecessors and affected the Rapaki village.

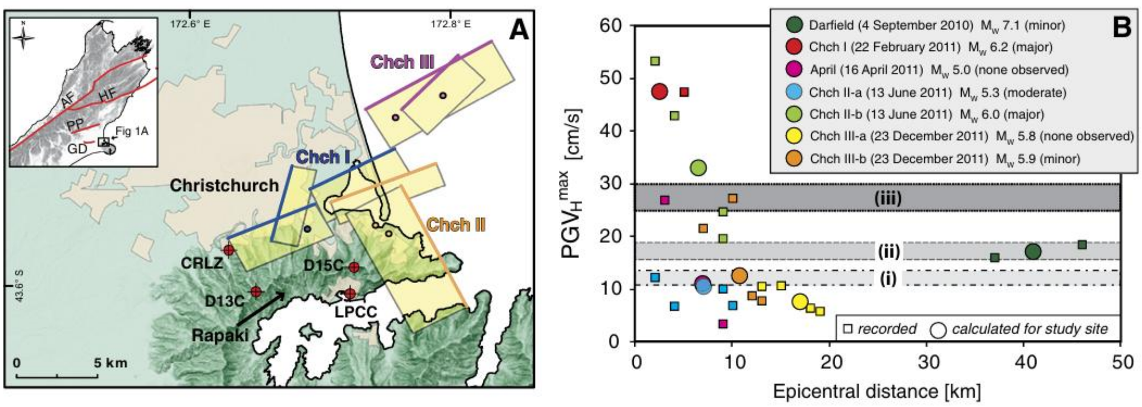

Figure 1. A: Christchurch, New Zealand, area showing location of Rapaki study site and blind fault sources (circles represent epicenters; shaded box is the fault plane; thick line shows surface projection of top of fault) from major 2011 earthquakes (Beavan et al., 2012). Chch I, II, and III are Christchurch earthquakes (see text). Seismic stations: LPCC—Lyttelton Port Company, D15C—Summit Road, D13C—Sign of the Kiwi, CRLZ—Canterbury Ring Laser. Inset shows northern South Island, with Alpine fault (AF), Hope fault (HF), Porters Pass fault (PP), and Greendale fault (GD) (the 2010 Darfield earthquake rupture). B: Processed instrumental maximum horizontal peak ground velocity (PGV_H^{max}) values for closest strong ground motion stations to the study site and estimated PGV_H^{max} at the rockfall source cliff plotted against epicentral distance for the strongest earthquakes (i.e., highest recorded PGVs) between A.D. 2010 and 2011 for which occurrence or nonoccurrence of rockfall is known. M_w—moment magnitude. Rockfall PGV_H^{max} triggering thresholds i–iii are described in text.

Relationship between ground motion intensity and rockfall severity. We estimated PGVH max at the source cliff for the strongest earthquakes using linear interpolation between the most proximally recorded PGVs (Fig. 1C). On the basis of rockfall observations and PGVH max calculations, we propose a rockfall triggering threshold of PGVH max = 12 ± 1 cm/s for the localized detachment of susceptible rocks in a previously fractured rock mass (minor to moderate PGVH max rockfall threshold; i in Fig. 1B), PGVHmax = 17 ± 2 cm/s for localized rock fracture and rockfall in an intact rock mass (ii in Fig. 1B; e.g., the Darfield earthquake), and PGVH max ≥ 25–30 cm/s for extensive rockfall and rock mass fracturing (iii in Fig. 1B; e.g., the Christchurch I earthquake). Variations in geology, elevation, and topography among seismometer sites contribute uncertainty to PGVH max estimates.

STOP 2: Sumner cliff collapse site (Duffy Lead)

STOP 2: Sumner cliff collapse site

1) Purpose and learning outcomes

This field trip examines earthquake-induced coastal and urban cliff collapse in the Sumner–Redcliffs sector of eastern Christchurch during the 2010–2011 Canterbury Earthquake Sequence (CES), with emphasis on rock-mass response, failure mechanisms, runout behaviour, and implications for land-use planning and risk management.

By the end of the trip, participants should be able to:

- Identify dominant **cliff-collapse mechanisms** (planar sliding, wedge failure, toppling, rockfall–avalanche behaviour) triggered by strong ground motion during the CES.
- Relate **lithology, rock-mass structure, and weathering** of the Port Hills volcanics to spatial variability in collapse style and magnitude.
- Distinguish **coseismic cliff collapses** from pre-CES slope failures using geomorphic freshness, talus morphology, and damage patterns.
- Critically evaluate how cliff-collapse inventories were translated into **red-zone land-use decisions** and long-term risk tolerability frameworks.

---

2) Cultural context and fieldwork protocol

The Sumner–Redcliffs area lies within the rohe of Ngāi Tahu, adjacent to Te Poho o Tamatea (Port Hills) and coastal environments of Whakaraupō and Pegasus Bay. Many collapse sites are immediately upslope of residential neighbourhoods affected by loss of life, property damage, and managed retreat.

Field protocol:

- Treat all sites as **post-disaster landscapes with cultural and social sensitivity**.
- Access only **public roads, beaches, and designated walkways**; do not enter fenced or red-zoned areas.
- No sampling, climbing, or approach to unstable cliff bases.
- Maintain awareness of rockfall risk from residual instability and marine undercutting.

---

3) Safety and risk management (critical)

Cliff collapse remains an ongoing hazard in the Sumner–Redcliffs area due to:

- Progressive rock-mass damage from CES shaking,
- Weathering and rainfall infiltration,
- Marine erosion at cliff toes.

Safety requirements:

- Maintain significant stand-off distances from cliff bases.
- Avoid overhanging sections and talus cones.
- Conduct visits only in dry, calm conditions with good visibility.

- Follow Christchurch City Council (CCC) hazard signage and exclusions.

---

4) Geological and geomorphic setting

The Sumner cliffs expose **Miocene Port Hills volcanic sequences**, including:

- Coherent basaltic lava flows,
- Volcanic breccias and agglomerates,
- Interbedded scoria and weakly welded pyroclastics.

Rock-mass behaviour is strongly controlled by:

- Steep coastal and urban escarpments,
- Persistent joint sets and cooling fractures,
- Lithologic contrasts producing strength anisotropy,
- Long-term marine and subaerial weathering.

These conditions preconditioned the cliffs for widespread collapse under CES ground motions.

---

5) Field itinerary and stops (expert focus)

Stop 2A — Clifton Terrace / Main Road Sumner: "Urban cliff collapse at the housing interface"

Theme: Direct interaction between cliff failure and residential exposure.

Observations

- Large coseismic cliff collapses that destroyed or severely damaged dwellings during the 22 February 2011 Mw 6.2 earthquake.
- Fresh head scarps, blocky talus, and disrupted retaining structures.
- Evidence of translational and wedge-controlled failures.

Discussion

- Why were these slopes marginally stable prior to 2011?
- How did shaking intensity and directionality amplify failure at this location?

Practitioner exercise

- Conduct a rapid qualitative rock-mass rating: joint spacing, persistence, orientation relative to slope face, and inferred failure modes.

Stop 2B — Redcliffs School / Moncks Bay margin: "Coseismic damage and legacy instability"

Theme: Persistence of hazard beyond the earthquake

Observations

- Ongoing rockfall and minor collapses years after the CES.
- Open fractures and tension cracks at cliff crests.
- Evidence for reduced rock-mass strength and fatigue.

Discussion

- How should post-earthquake degradation be incorporated into long-term hazard models?
- What constitutes an acceptable residual risk in urban cliff environments?
- Potential to considered variations in risk tolerance for different types of buildings?

Summary Implications for hazard, zoning, and risk governance

The Sumner–Redcliffs cliff collapses were central to Christchurch's post-CES risk policy evolution, including:

- Establishment of **residential red zones**,
- Explicit adoption of **risk-based land-use planning**,
- Integration of empirical collapse inventories with probabilistic hazard assessment.

For practitioners, these sites illustrate:

- Limits of pre-event hazard mapping,
- Importance of conservative treatment of steep volcanic cliffs,
- The necessity of coupling geologic insight with transparent societal risk thresholds.

REFERENCES

Bradley, B. A., Quigley, M. C., van Ballegooy, S., Lan, C., & Baker, J. W. (2014). Ground motion and site effects observed in the 2010–2011 Canterbury earthquakes. Earthquake Spectra, 30(1), 1–27. https://doi.org/10.1193/021913EQS050M

Christchurch City Council. (2014). Port Hills slope stability: Summary of rockfall and cliff collapse hazard and risk. Christchurch, New Zealand.

Massey, C. I., Della Pasqua, F., Holden, C., Kaiser, A., Richards, L., Wartman, J., McSaveney, M., & Archibald, G. (2018). Rock slope response to strong earthquake shaking. Landslides, 15(12), 2495–2513. https://doi.org/10.1007/s10346-018-1063-0

Quigley, M. C., Hughes, M. W., Bradley, B. A., van Ballegooy, S., Reid, C., Morgenroth, J., Horton, T., Duffy, B., & Pettinga, J. R. (2016). The 2010–2011 Canterbury Earthquake Sequence: Environmental effects, seismic triggering thresholds and geologic legacy. Tectonophysics, 672–673, 228–274. https://doi.org/10.1016/j.tecto.2016.01.044

Quigley, M. C., Saunders, W., Massey, C., Van Dissen, R., Villamor, P., Jack, H., and Litchfield, N.: The utility of earth science information in post-earthquake land-use decision-making: the 2010–2011

Canterbury earthquake sequence in Aotearoa New Zealand, Nat. Hazards Earth Syst. Sci., 20, 3361–3385, https://doi.org/10.5194/nhess-20-3361-2020, 2020.

Townsend, D. B., Rosser, B. J., Allen, S. K., & Kaiser, A. E. (2016). Assessing landslide hazard in New Zealand: A review of recent developments. New Zealand Journal of Geology and Geophysics, 59(2), 195–214. https://doi.org/10.1080/00288306.2016.1152623

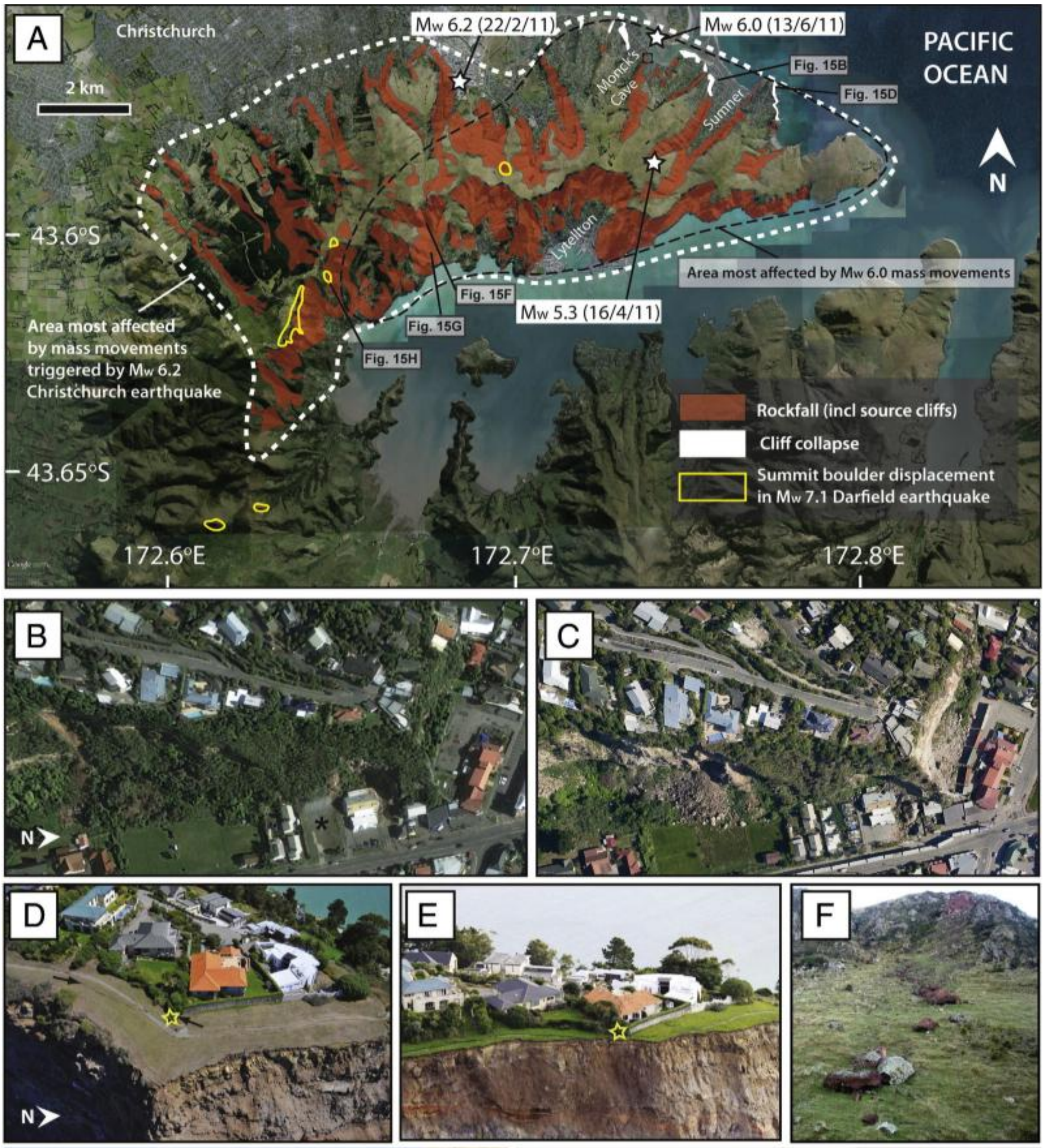

Selected images and maps of CES rockfall, cliff collapse, and boulder displacement. (A) Spatial distribution of rockfall, cliff collapse and summit boulder displacements in the Port Hills south of Christchurch resulting from different CES earthquakes. Boundary of areas most affected by M_w 6.2 and 6.0 Christchurch earthquakes adopted from Massey et al., 2014. (B) Aerial photograph from 4 Sept 2010 immediately following the M_w 7.1 Darfield earthquake. Note unvegetated bedrock slopes, *indicating (pre-earthquake) slope instability. Note vacant lot indicated by *. Despite high rates of seismicity following the M_w 7.1 Darfield earthquake, future residential development took place near base of cliffs. (C) Aerial photograph of same area as (B) showing cumulative cliff collapse and rockfall effects induced by the M_w 6.2 and 6.0 Christchurch earthquakes. Photo taken 26 April 2012. Note rockfall in inhabited areas and consequent abandonment of uncompleted residential complex. (D) Aerial photograph taken by lead author 3 days following the M_w 6.2 Christchurch earthquake (25 Feb 2011), showing incipient surface fissuring approximately 15 m from bedrock cliff edge (denoted with arrows) in residential area. (E) Photo of same area as (D) by R. Van Dissen (GNS Science) following Mw 6.0 Christchurch earthquake, showing deep seated bedrock cliff collapse using detachment surface shown by incipient failure cracks in (D). (F) Rockfall and rock slides in the Port Hills resulting from the M_w 6.2 and 6.0 Christchurch earthquakes. Note presence of fallen rock debris with the formerly-exposed surface facing up, and formerly unexposed surfaces facing up, highlighting the challenges of using surface exposure age dating techniques (e.g. Mackey and Quigley, 2014) to date paleo-rockfall deposits. Note bedrock source cliff, identifiable by red-coloured unweathered volcanic bedrock, near top of the hillslope.*

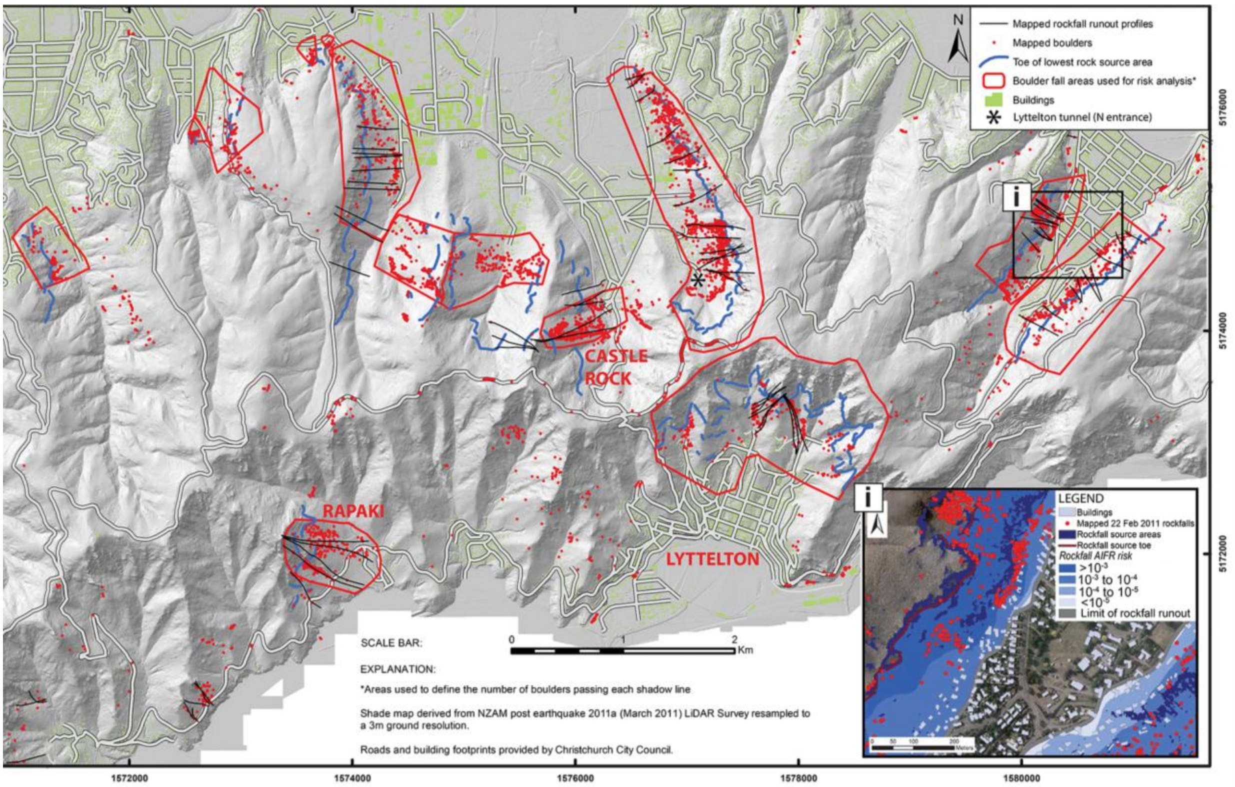

Mapped mass movement hazards (rockfall boulders and source areas, boulder runout trajectories, and areas used for rockfall risk analyses) shown relative to infrastructure (roads – white lines, buildings – green shade) in the Port Hills area of southern Christchurch. Base image is lidar digital elevation model (DEM) hillshade with 3 m resolution. Inset (i): example of annual individual fatality risk (AIFR) contour map used for decision-making. Figure and inset modified from Massey et al. (2012).

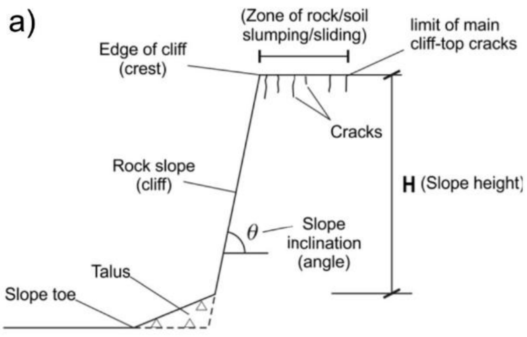

Summary of the geometry and rock fall volumes triggered by the 22 February–13 June 2011 earthquakes from the large and major slopes. (a) Schematic diagram showing the dimensions of the slopes used in this analysis;

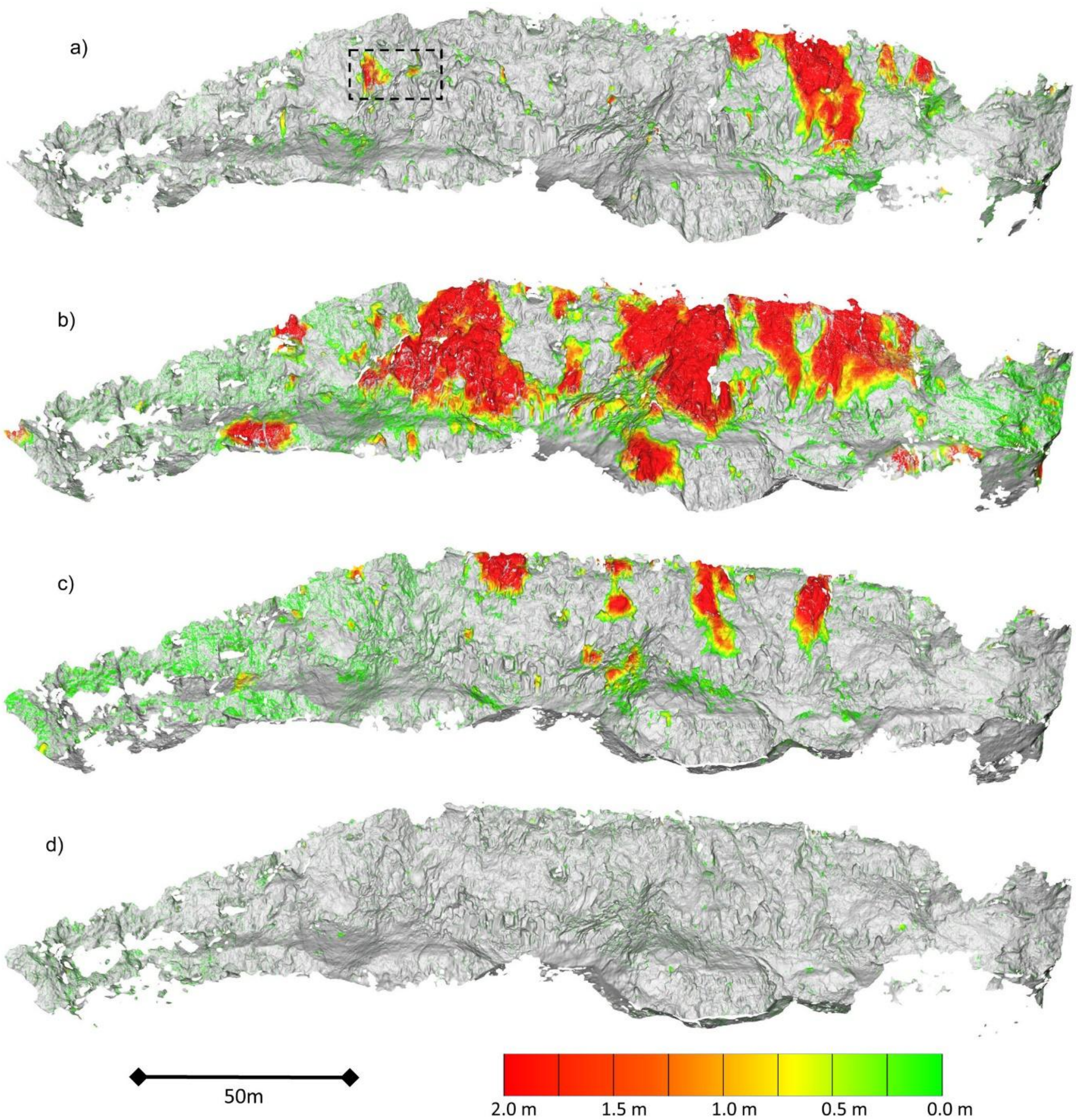

*Example surface change model for the Redcliffs Southwest sub slope. The views are the frontal elevations of the Redcliffs Southwest slope surface (gray hillshade tin model) viewed looking onto the slope where the y-axis is the elevation above the toe of the slope. The y- and x-axes are equal in scale. The colors show the negative surface change (erosion) between survey epochs above a change threshold of 0.05 m only, between (a) 3/6/2011 and 5/3/2011, (b) 5/3/2011 and 6/15/2011, (c) 6/15/2011 and 1/18/2012, and (d) 1/18/2012 and 5/1/2012. The cell size is 0.1 m for this analysis. The dashed black rectangle shows the location of Figure **11**.*

Photographs showing the major slopes in this study. (a) Shag Rock Reserve (Peacock's Gallup), taken during the 14 February 2016, earthquake (Photo Credit: Stuff). (b) Redcliffs taken after the 22 February 2011 earthquake (Photo Credit: G.T. Hancox). (c) Wakefield and Nayland, taken after the 22 February 2011 earthquake (Photo Credit: G.T. Hancox). (d) Redcliffs Road, taken after the 13 June 2011 earthquake. (e) Shag Rock Reserve, taken after the 13 June 2011 earthquake. (f) Whitewash Head, taken after 13 June 2011 earthquake.

STOP 3 Coastal settings of eastern Christchurch: Bridge Street Reserve (Catherine Reid)

1) Purpose and learning outcomes

This field stop examines **liquefaction and subsidence impacts** in the Avon-Heathcote Estuary | Ihutai (AHEI) during the 2010–2011 Canterbury Earthquake Sequence (CES) and discusses the geological **evidence for** vertical deformation in soft sediment settings. The itinerary is designed for expert practitioners and emphasizes process interpretation, stratigraphic/geomorphic context, and implications for hazard and risk governance, drawing particularly on the work of **Reid and Quigley** (e.g., Quigley et al., 2016; Reid et al., 2017) and related CES subsidence mapping and paleoliquefaction assessments (e.g., Hughes et al 2015).

By the end of the trip, participants should be able to:

- Identify modern field features that may indicate vertical deformation and appreciate the drivers of sedimentation or erosion in vegetated inter-tidal zones
- Explain the capacity of coastal settings to record palaeoseismic deformation (Quigley et al., 2016).

2) Cultural context and fieldwork protocol

The Avon-Heathcote Estuary | Ihutai lies at the terminus of the Ōtākaro (Avon River) within a long-utlised cultural landscape. Many localities remain socially sensitive because of red-zoning, displacement, and ongoing river-corridor regeneration.

Field protocol:

- Use public access points (e.g., river corridor paths, bridges, road reserves). Do not enter fenced or restricted areas.
- No excavation/sampling. If you intend to examine subsurface expression, do so via existing published trench logs and exposures rather than new disturbance (Bastin et al., 2015).

3) Safety considerations

Primary hazards include:

- Soft ground on tidal mudflats
- Incoming tide (Low-tide within the estuary approximately 2.30pm)
- Slips/trips in riparian zones and after rainfall.

High-visibility clothing is recommended near roads; avoid riverbank edges where undermined or recently regraded.

4) Setting:

The AHEI is a tide dominated coastal estuary with freshwater and muddy sediment input from the Avon and Heathcote rivers. The bulk of the sandy material is derived from coastal settings. During the CES the AHEI experienced both vertical deformation and significant liquefaction. It became a natural laboratory to investigate the preservation of these features in the geological record

5) Field itinerary and stops

Bridget Street overview:

Theme: The record of subsidence of an inter-tidal saltmarah.

What to observe

- Salt-marsh inundation of previous supratidal setting.

- Inter-tidal plant zonation and their implications for sediment trapping - wave attenuation

Practitioner exercise

- Sketch a rapid inter-tidal plant and geomorphic cross section. Mark on approximate vegetation height. Consider, with respect to tidal inundation and plant height where you would anticipate erosion or sediment and deposition of sediment.

Discussion: The AHEI demonstrated key features relevant to interpreting palaeoseismic events in soft sediment estuarine settings:

1. Estuarine settings are more susceptible to soft sediment compaction and this has major implications for interpretation of the geological record.
2. Interpretation of the palaeoseismic record needs to be informed by relative sediment supply and erosion dynamics at any study site.

AVON-HEATHCOTE ESTUARY DEFORMATION

The Avon-Heathcote/Ihutai Estuary (AHEI) is a tidally dominated estuary isolated from the sea by the Brighton Spit, with the Avon River feeding into it in the north, and the Heathcote River to the southwest. The AHEI is bound on its southern edge by the volcanic rocks of Banks Peninsula, but all other shore lines are bound by uncompacted sands and silts. The AHEI is presently thought to have formed about 450 years ago (Owen, 1992, McFadgen and Goff, 2005) determined on the basis of geomorphic principles and adjacent cave deposits. This is currently being tested by postgraduate student research utilising long cores from within the estuary collected for rebuild geotechnical purposes.

Geographic features of the Avon-Heathcote/Ihutai Estuary and the survey sites osed to assess deformation and biotic response to coseismic deformation by Reid, Cochran, Clark and Marsden.

Urban settlement around the AHEI began in the mid 1800's on its southern shore, with much of the north-western portion rural into the 1900's. New Brighton town-ship was developing from the late 1800's but the southern half of Brighton Spit only began to be settled in about 1940, and there is conjecture that the spit may have been open, or partially open at Caspian St (Findlay and Kirk, 1988). The AHEI supports a rich ecological system (Jones and Marsden 2005) but has been impacted by the urbanisation of Christchurch firstly with industrial and urban untreated waste from the 1800's and latterly with treated sewage outfall from the Bromley sewage treatment plant. The Bromley sewage outfall pipe finally bypassed the AHEI in early 2010 and the outfall pipe now discharges treated effluent offshore into Pegasus Bay. During the CES damage to underground services and the Bromley plant resulted in short-term discharge of raw sewage into the AHEI following the mainshock and each of the major aftershocks.

Sand volcanoes in the Estuary Rd area produced by the 13th June 2011 aftershocks prior to removal by wave and tide action.

The September 2010 mainshock and each of the major aftershocks resulted in widespread development of sand volcanoes in the AHE (Fig. 10 and 11) and these were most pronounced following the February 2011 event (Reid et al. 2012). The record of these sand blows is now largely removed by tidal and wave activity, although remnants of the larger cones remain in sheltered areas (these can be seen at Bridge St). The sand introduced to the Estuary has largely been reworked rather than removed and the floor of the middle AHE has been raised both by tectonic deformation and the retention of fine sand introduced following liquefaction (Measures et al 2011). In places broad low sand bars remain where following the February and June events large (7-8m diameter) sand blows were seen. Elsewhere sand introduced by liquefaction can be seen as a redistributed veneer over mud or sandy mud pre-CES surfaces.

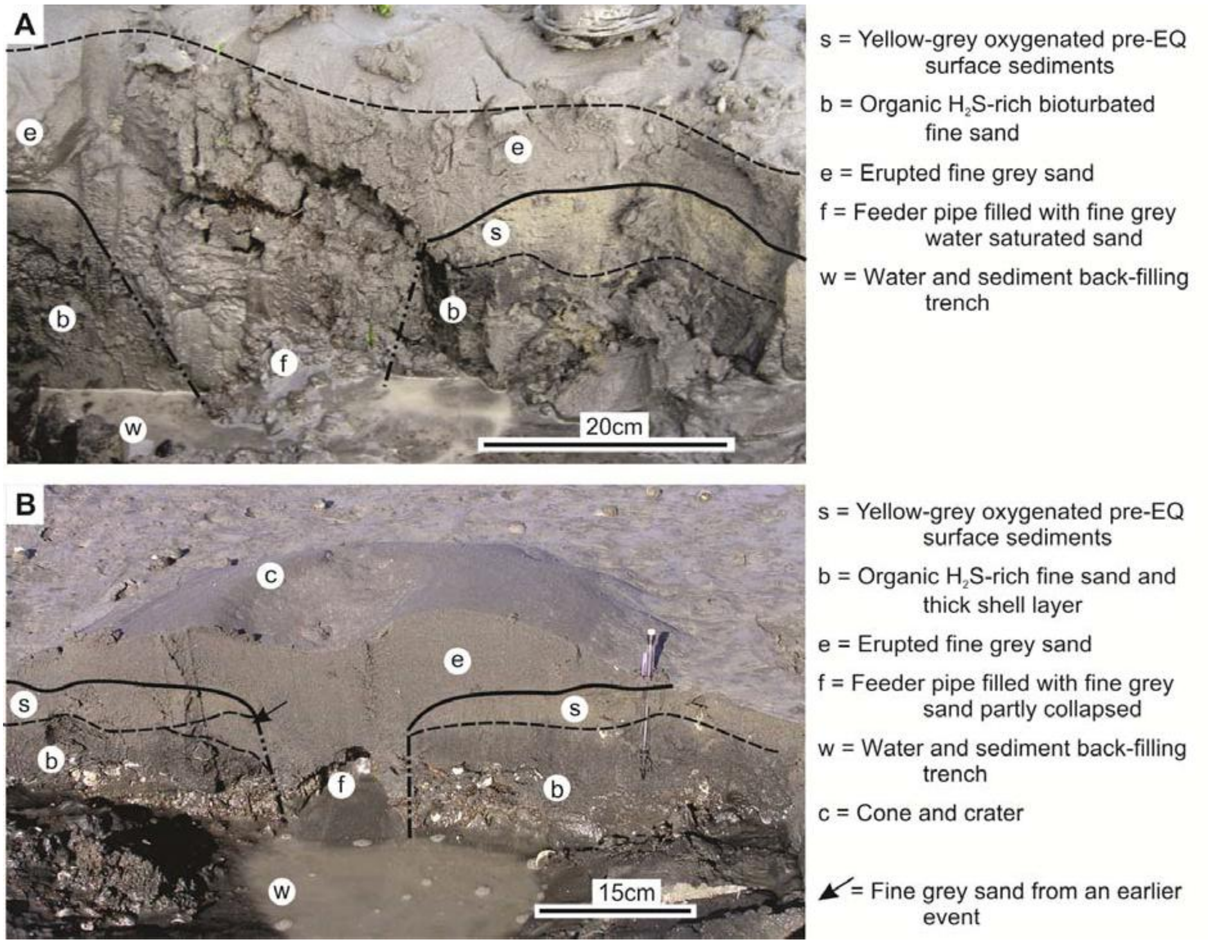

Cross sections through sand volcanoes of the Sept 4th (A) and June 13th (B) earthquakes. From Reid et al (2012).

The February 22nd event on what is now termed the Port Hills fault also resulted in vertical ground deformation in the AHEI. The southern portion has been uplifted and the northern portion has experience significant subsidence. This deformation is the sum of both tectonic (uplft and subsidence) and soft-sediment (subsidence) deformation. LiDAR data (Fig. 12) shows up to 40cm of uplift on the AHEI southern margin of volcanic rock, and variably 20-30cm in land areas underlain by sands and silts. This differential uplift is the result of tectonic uplift minus soft sediment compaction. In the northern AHEI subsidence is pronounced and is the result of the combination of tectonic subsidence and soft sediment compaction.

The response of plant and microflora and fauna to coseismic deformation iwas studied by a collaborative team from UC and GNS. Three monthly surveys from June 2011 to 2014 have revealed progressive shift of macroflora, using the tidal height sensitive plant *Sarcocornia* (glasswort) as a marker of deformation (Reid et al 2017).

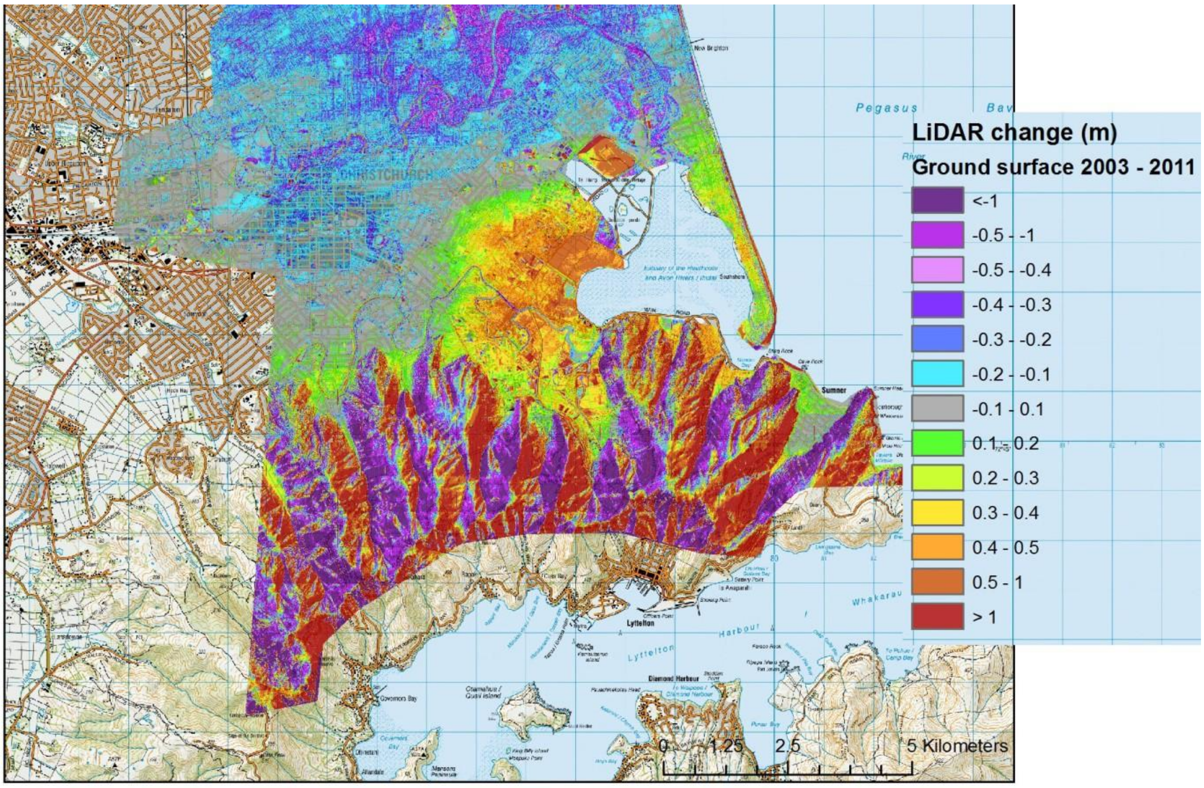

LiDAR data courtesy AAM (2003) and NZAM (2011).
2003 survey commisioned by Christchurch City Council, 2011 survey commisioned by MCDEM.

LiDAR map of eastern Christchurch showing ground deformation associated with the February 2011 EQ. Strong colours on the Port Hills reflect horizontal not vertical deformation.

BRIDGE ST RESERVE

This area of the AHE has experienced significant subsidence as a result of the February 2011 EQ and part of the reserve on the northern side of Bridge St has been used as a survey site to monitor plant, sediment and microbiota response to deformation (Fig. 13). The key plant in the study is the glasswort *Sarcocornia* that in the AHE is a reliable larker of High Spring Tide (HST) (Islay Marsden pers comm. 2011). In the Bridge St site the *Sarcocornia* has shifted landward in response to subsidence. Although a new HST boundary for *Sarcocornia* has yet to establish itself, 3-monthly measurements of HST heights, and the erosion line marked on the stop-bank, indicate approximately 45 cm of subsidence here.

SETTLERS RESERVE

The southern portion of the AHE has experienced uplift and at Settlers Reserve this is evidenced in a seaward shift of *Sarcocornia* plants (Fig. 14). Landward plants are in poor health and are being invaded by grasses and other plants but have not died off as dramatically as at Bridge St, assumed to be a response to existing salt in soils and occasional wetting in flood events coincident with high spring tides.

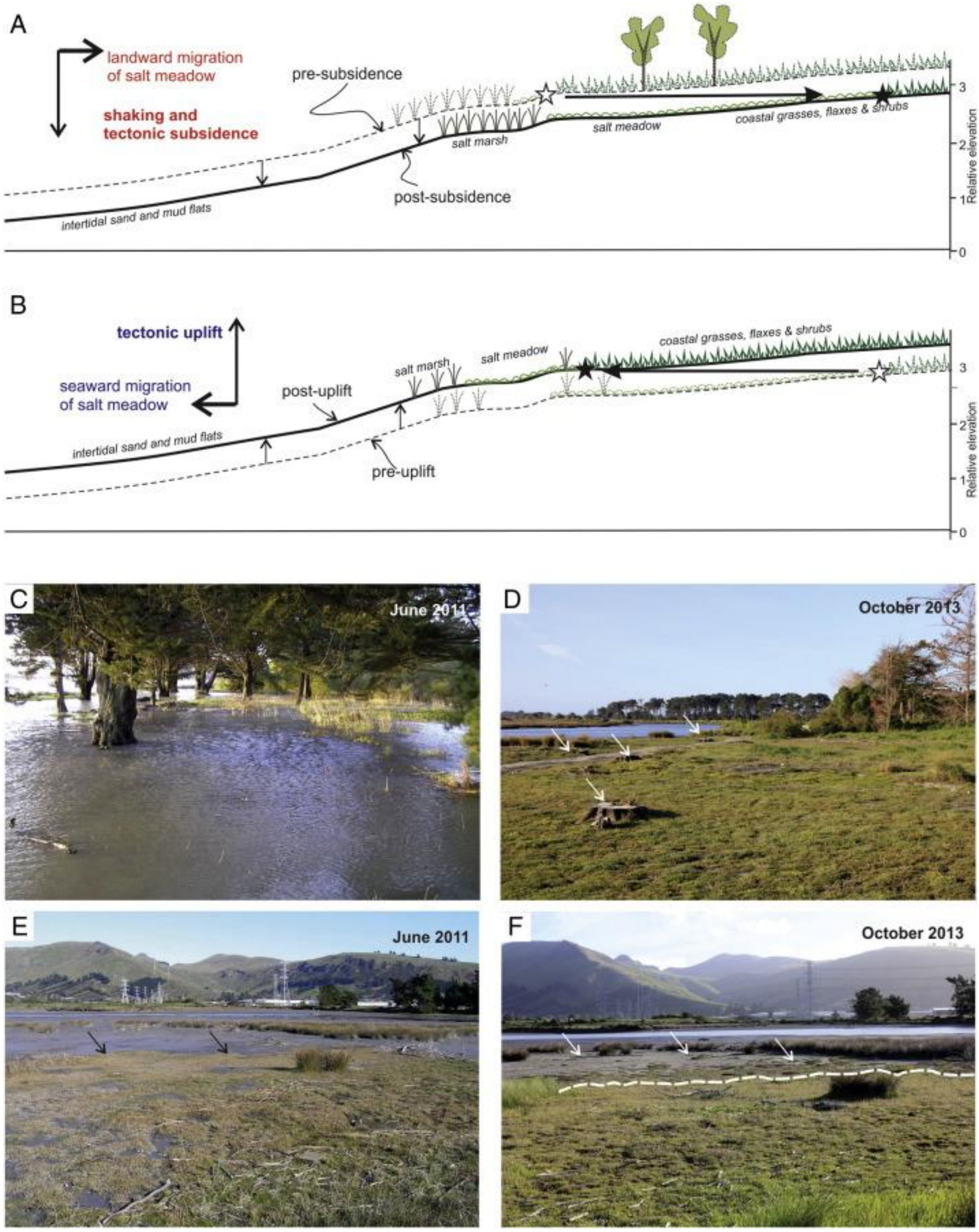

Response of estuarine salt meadow to ground deformation. (A–B) Schematic representation of typical tidal zonation of salt meadow, salt marsh and inter-tidal flats in southern New Zealand, and migration of those zones in response to deformation. Stars indicate relative change of position of saltmarsh boundary with deformation, dashed line indicates schematic pre-deformation ground position, elevation changes are representative. (A) Migration of tidal plant zones in response to subsidence (see C–D for field images). (B) Migration of tidal plant zones in response to uplift (see E–F for field images). (C) Bridge Street reserve in the northern estuary in 2011, following subsidence, showing inundation of coastal plant zone at high spring *tide; tide is covering grasses and plants that normally grow above high spring tide. (D) Same site in October 2013, taken at a lower tide after two growing seasons, showing migration of salt meadow plants landward to surround stumps of pre-deformation large trees (arrows). (E) Southern estuary site in June 2011 following uplift with salt meadow still representing a pre-deformation position, seaward edge of the salt meadow arrowed. (F) Same site in October 2013 after two growing seasons and the migration of salt meadow plants seaward (arrows) in response to uplift. Dashed line indicates margin of pre-deformation salt meadow.*

REFERENCES

Hayward, B. W., Sabaa, A. T., Figueira, B., Reid, C. M., & Nomura, R. (2015). Foraminiferal record of the 2010–2011 Canterbury earthquake sequence, New Zealand, and possible predecessors. *Palaeogeography, Palaeoclimatology, Palaeoecology*, *438*, 213-225.

Hughes, M. W., Quigley, M. C., van Ballegooy, S., Deam, B. L., Bradley, B. A., & Rhoades, D. A. (2015). The sinking city: Earthquakes increase flood hazard in Christchurch, New Zealand. GSA Today, 25(3), 4–10. https://doi.org/10.1130/GSATG221A.1

Quigley, M. C., Hughes, M. W., Bradley, B. A., van Ballegooy, S., Reid, C., Morgenroth, J., Horton, T., Duffy, B., & Pettinga, J. R. (2016). The 2010–2011 Canterbury Earthquake Sequence: Environmental effects, seismic triggering thresholds and geologic legacy. Tectonophysics, 672–673, 228–274. https://doi.org/10.1016/j.tecto.2016.01.044

Reid, C. M., Thompson, N. K., Irvine, J. R. M., & Laird, T. E. (2012). Sand volcanoes in the Avon–Heathcote Estuary produced by the 2010–2011 Christchurch earthquakes: Implications for geological preservation and expression. New Zealand Journal of Geology and Geophysics, 55(3), 249–254. https://doi.org/10.1080/00288306.2012.674051.

Reid, C., Cochran, U., Clark, K., Marsden, I., Litchfield, N., & Ries, W. (2017). Salt marsh plant response to vertical deformation resulting from the February 2011 Christchurch earthquake. New Zealand Journal of Geology and Geophysics, 60(3), 220–238. https://doi.org/10.1080/00288306.2017.1307233

STOP 4: AVONSIDE: Liquefaction at Porritt Park (Bastin and Duffy leads)

STOP 5: Porritt Park Liquefaction (*Brendan Duffy lead*)

At this stop, we will consider the importance of buried geomorphology and will also pay some attention to the effects of anthropogenic activity on liquefaction effects. The area is located adjacent to the Avon River, with Porrit Park comprising an anthropogenically cut-off meander bend. Porrit Park and the wider Avondale area generally experienced severe liquefaction during the CES. Twith lateral spreading additionally occurring towards the Avon River.

Areas with severe liquefaction were generally found to contain shallow groundwater levels (<1m) and underlain by loose fluvial sands and silts. These deposits are known to be highly susceptible to liquefaction. On Emlyn Place (A on map below), a narrow zone in the middle of the street did not liquefy and houses suffered relatively little damage. Observations under houses in the middle of this street shows that they are built on sand, likely comprising dune sands that are exposed further east of Wainoni Road. The higher density clean dune sand is considered less susceptible to liquefaction than the surrounding fluvial sands and silts which are present elsewhere in the street.

On Avonside Drive nearby, a west-side-down lateral spread scarp trends NS and projects across a recently (artificially) abandoned meander of the Avon River (LS1 on map below). The scarp is not obvious in Porritt Park, within the meander, but a swamp formed in a depression on the line of the lateral spread (B on map below). A continuation of what appears to be the same scarp picks up on the south side of the meander (LS2 on map below), curving sub-parallel with the river. The geomorphology relative to the river is (almost?) indistinguishable from a terrace. Topics for discussion include:

- Is the lateral spread, with its unusual geometry, formed along a buried river bank, implying that buried geomorphology controlled the landward limit of spreading?
- Would that feature, in the absence of a priori knowledge, be considered a paleoseismic feature (lateral spread) or a river terrace?
- What drives the complete infilling of the channel complex? Subsidence? Mid-Holocene high stand?

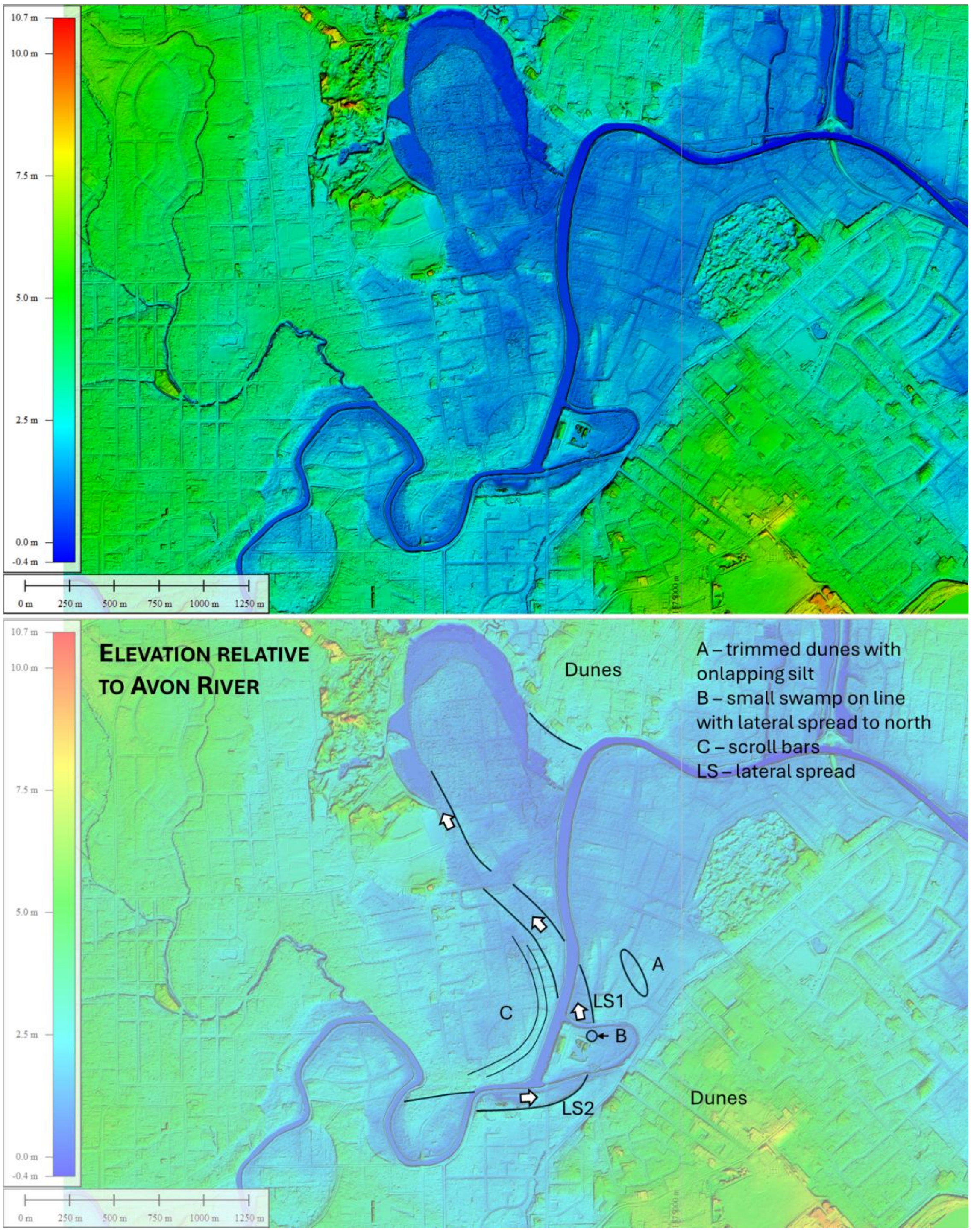

Relative elevation map, showing the apparent trace of buried channels defining a previous course of the Avon River, now associated with lateral spreading at the paleo-river banks

Another interesting aspect of Stop 5 is the influence of progressive anthropogenic land modifications on the surface expressions of liquefaction and lateral spreading during the CES. The figures below highlight landscape modifications over the time periods shown (from Borella et al., 2020). The spatial patterns and severity of liquefaction and lateral spreading in the CES was strongly influenced by landscape engineering and infrastructure. See images below.

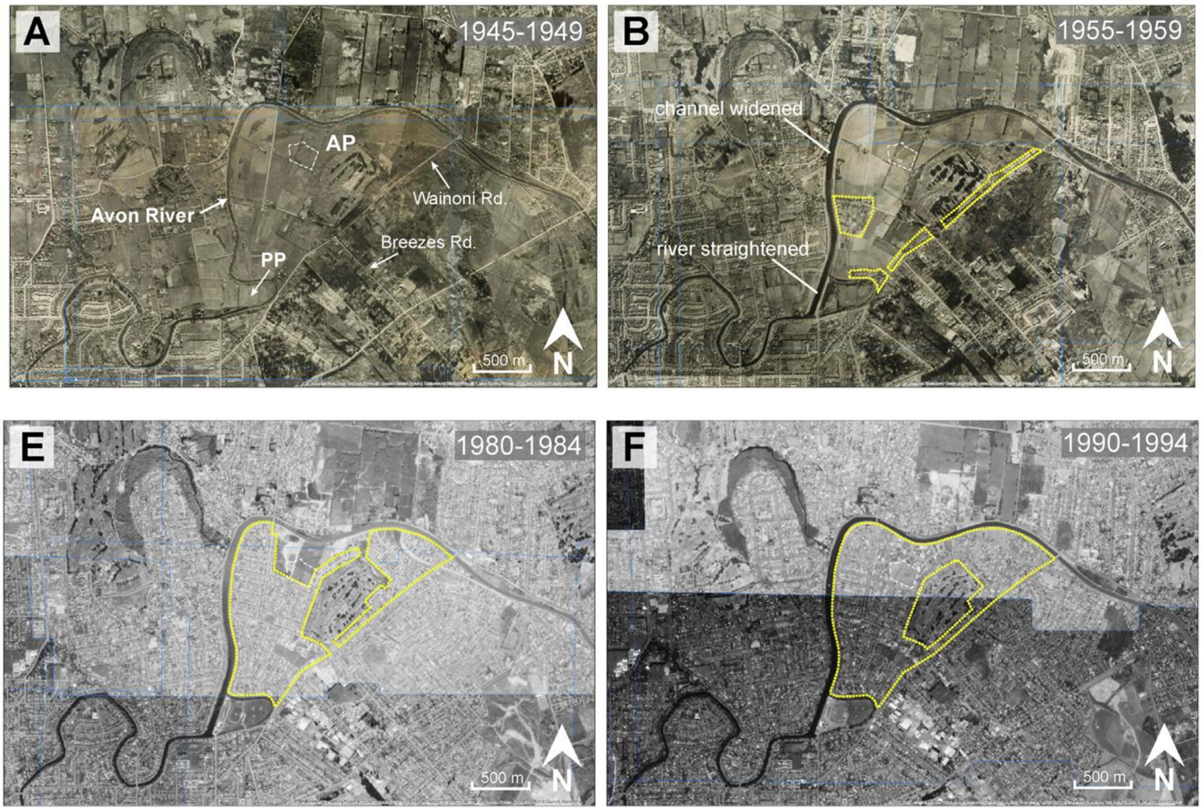

Historical aerial photographs highlighting the sequence (A–F) of anthropogenic modifications near Avondale Park, Porritt Park, and surrounding residential areas.

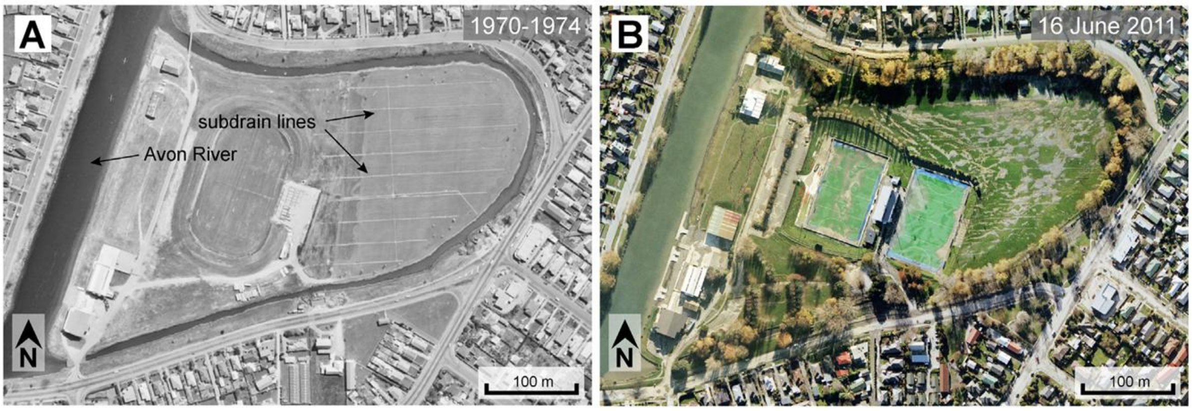

(A) Porritt Park before CES: 1970–1974 historical aerial photographs showing East-West oriented subdrain system. (B) Porritt Park after CES: Aerial photograph taken on 16 June 2011, a few days after the 13 June 2011 earthquake. Note the locations for the pre-existing subdrain lines and distribution of liquefaction ejecta

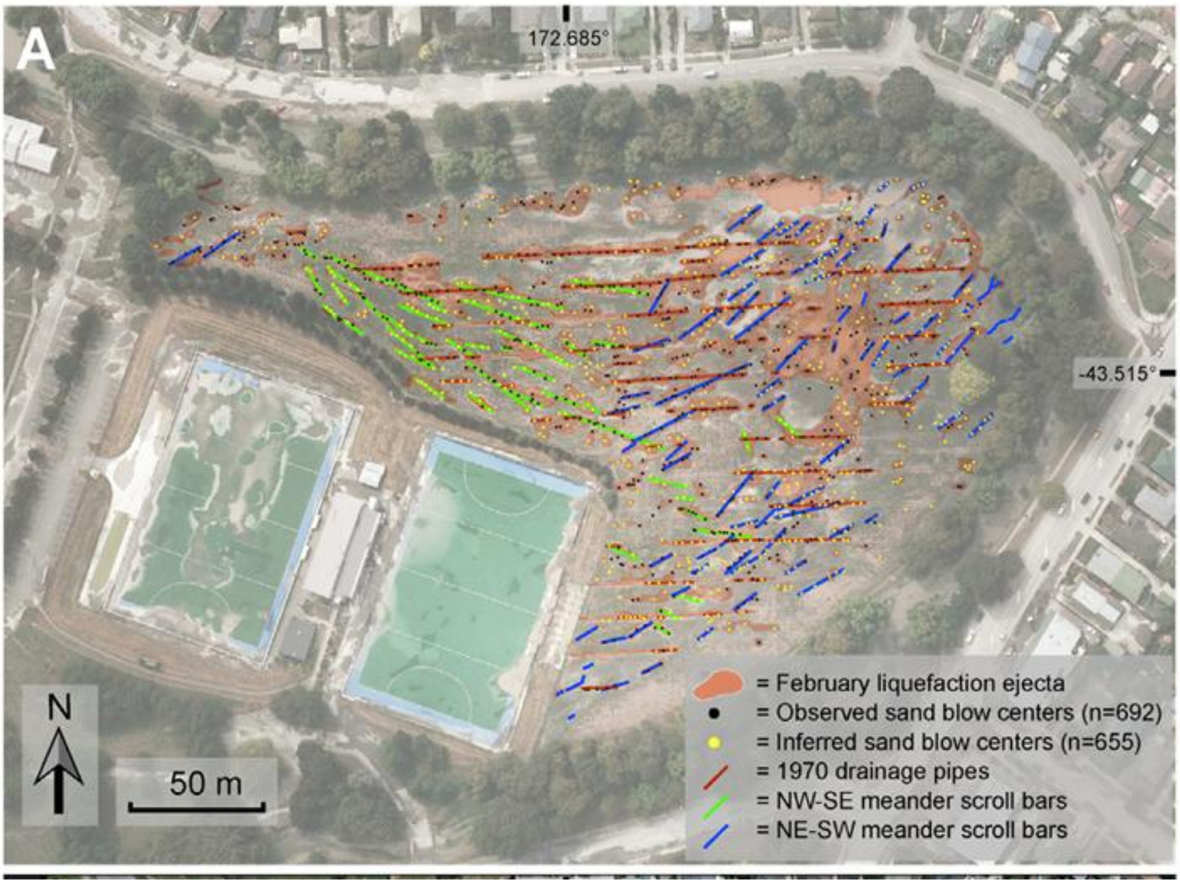

Liquefaction ejecta (red polygons) at Porritt Park during the 22 February 2011 earthquake

<u>REFERENCE FOR STOP 5:</u>

Borella, J., **Quigley, M.**, Riley, M., Trutner, S., Jol, H., Borella, M., Hampton, S., Gravley, D., (2020) Influence of anthropogenic landscape modifications and infrastructure on the geological characteristics of liquefaction, *Anthropocene, v.* 29, 100235

https://www.drquigs.com/wp-content/uploads/2020/09/1-s2.0-S2213305420300011-main.pdf

STOP 5: AVONSIDE: Liquefaction in inner meander of Avon River (Quigley and Bastin leads)

Field trip guide: Liquefaction impacts and evidence for paleoliquefaction in Avonside, eastern Christchurch (Canterbury Earthquake Sequence)

---

1) Purpose and learning outcomes

This field trip examines **recurrent liquefaction impacts** in Avonside (eastern Christchurch) during the 2010–2011 Canterbury Earthquake Sequence (CES), and the **field evidence for paleoliquefaction** preserved beneath and adjacent to modern liquefaction features. The itinerary is designed for expert practitioners and emphasizes process interpretation, stratigraphic/geomorphic context, and implications for hazard and risk governance, drawing particularly on the work of **Quigley and Bastin** (e.g., Quigley et al., 2013; Bastin et al., 2015) and related CES liquefaction mapping and paleoliquefaction assessments (e.g., Townsend et al., 2016; Villamor et al., 2016).

By the end of the trip, participants should be able to:

- Diagnose **liquefaction manifestation styles** in an urban floodplain setting (sand blows, fissure-aligned sand ridges, blisters/injected sills, lateral spreading, settlement) and link them to subsurface conduit architecture (Quigley et al., 2013; Villamor et al., 2016).
- Explain why Avonside experienced **recurrent liquefaction** (multiple events reactivating the same vent/fissure network) and how this changes land-damage trajectories over a sequence (Quigley et al., 2013).
- Identify field and subsurface criteria that differentiate **paleoliquefaction** from CES features (cross-cutting relationships, pedogenic alteration, infilling and truncation, stratigraphic context, preservation potential) (Bastin et al., 2015; Villamor et al., 2016).
- Translate site observations into **practitioner-relevant implications** for liquefaction susceptibility mapping, microzonation, and land-use planning (Townsend et al., 2016; Hughes et al., 2015).

---

2) Cultural context and fieldwork protocol

Avonside lies along Ōtākaro (Avon River) within a long-occupied cultural landscape. Many localities remain socially sensitive because of red-zoning, displacement, and ongoing river-corridor regeneration.

Field protocol:

- Use public access points (e.g., river corridor paths, bridges, road reserves). Do not enter fenced or restricted areas.
- No excavation/sampling. If you intend to examine subsurface expression, do so via existing published trench logs and exposures rather than new disturbance (Bastin et al., 2015).
- Treat the suburb as an **urban disaster-scape**: be respectful of residents, memorials, and recovery works.

---

3) Safety considerations

Primary hazards are not cliff-based, but include:

- Unstable riverbanks and soft ground where liquefaction and reworking occurred.
- Traffic exposure at bridge/road stops.
- Slips/trips in riparian zones and after rainfall.

High-visibility clothing is recommended near roads; avoid riverbank edges where undermined or recently regraded.

---

4) Setting: why Avonside is a liquefaction "type locality"

Avonside occupies a relatively low-lying area encompassed by a meander bend of the Avon River. The area hosts shallow groundwater (typically <1m) and is underlain by laterally variable **sandy channel and overbank sands and silts deposits** that are highly susceptible to liquefaction. The CES demonstrated that some sites liquefied repeatedly, producing compound deposits and multi-phase dike/vent development (Quigley et al., 2013). Paleoliquefaction investigations indicate that susceptible sites can preserve evidence of pre-CES liquefaction episodes, but preservation is strongly conditioned by geomorphic stability, sedimentation, and soil development and typically only subsurface features are preserved (Bastin et al., 2015).

---

5) Field itinerary and stops (expert practitioner focus)

Avon River corridor overview: "Geomorphic template controls manifestation"

Theme: Interpreting liquefaction within a floodplain–channel geomorphic framework.

What to observe

- Floodplain morphology and subtle relief that modulates where sand blows and fissures preferentially occur (scroll bars, abandoned channels, levee/backswamp contrasts) (Villamor et al., 2016).
- Lateral spreading susceptibility at channel margins (bank-parallel fissuring, ground cracks, and repaired bank treatments) (Cubrinovski & Green, 2010).

Practitioner exercise

- Sketch a rapid geomorphic cross-section: channel margin → levee/scroll-bar ridge → swale/backswamp. Predict which sub-environments should host (i) vents, (ii) fissure-aligned ridges, (iii) injected sills/blisters, and justify using CES observations (Villamor et al., 2016; Quigley et al., 2013).

Recurrent liquefaction exemplar locality: "Same site, multiple earthquakes, evolving land damage"

Theme: Repeated vent reactivation and compound sand blow construction.

What to observe (conceptual, using published mapping)

- Quigley et al. (2013) document a detailed Avonside study site where multiple CES events produced distinct sand blow footprints and cumulative sedimentation patterns, with reoccupation of the same conduit network across events (Quigley et al., 2013).

Key interpretive points

- Recurrent liquefaction is not simply “repeat occurrence”; it is a **system** of evolving permeability architecture (dikes, fissures, vent complexes) that can focus future manifestation at the same site while also modifying surface expression and vulnerability over time (Quigley et al., 2013).
- There is little to no observable surface evidence of the recurrent severe liquefaction during the CES however subsurface features remain. Trenching to identify features can constrain recurrence/ approximate timing of strong ground motions triggering liquefaction.

Practitioner exercise

- Using the Quigley et al. (2013) event-by-event footprint concept, discuss how you would encode “sequence effects” into (a) land performance zoning, and (b) asset fragility/repair prioritisation.

Subsurface expression and paleoliquefaction criteria: “How do we recognise older liquefaction beneath Avonside?”

Theme: Field criteria for paleoliquefaction in a disturbed urban floodplain.

Evidence framework (from published trenching and descriptions)
Bastin et al. (2015) show that paleoliquefaction can be identified beneath/adjacent to CES features using:

- Cross-cutting relationships: modern dikes that cut older, more altered dikes/sills.
- Pedogenic/weathering contrasts: older features show stronger oxidation, soil structure development, or infilling/compaction differences relative to sharp-edged CES dikes.
- Stratigraphic position and truncation: older dikes may be truncated by erosion surfaces or buried by overbank units prior to modern reactivation (Bastin et al., 2015).

Practitioner exercise

- Define a “minimum defensible” paleoliquefaction interpretation standard for Christchurch-type settings: what combination of (i) stratigraphic controls, (ii) alteration indicators, and (iii) independent dating/chronologic constraints would you require before you would use paleoliquefaction as a planning-grade input? (Bastin et al., 2015; Villamor et al., 2016)

Neighbourhood-scale geomorphic variability and land damage: “Why does Avonside vary block-to-block?”

Theme: Microgeomorphology, soil heterogeneity, topographic variability, and damage expression.

What to focus on

- Spatial non-uniformity of liquefaction-induced damage (differential settlement, lateral spreading intensity, infrastructure disruption) as a function of shallow stratigraphy and geomorphic setting (Townsend et al., 2016; Villamor et al., 2016).

Practitioner exercise

- Compare two nearby reaches (or blocks) in the mapped liquefaction dataset and propose a testable explanation for differences (e.g., scroll-bar ridge vs swale; variable sand thickness; groundwater depth). Use the mapping framework of Townsend et al. (2016) to support your reasoning.

Cascading hazards: subsidence, flood hazard, and long-term geomorphic adjustment

Theme: Liquefaction impacts that persist beyond the shaking.

Key concepts

- Liquefaction-induced settlement and lateral spreading contributed to persistent land-level lowering and altered drainage efficiency, elevating flood hazard in parts of eastern Christchurch (Hughes et al., 2015).
- For Avonside, this connects liquefaction to longer-term management issues (freeboard, stormwater performance, river corridor design), rather than treating liquefaction solely as an episodic "event damage" problem (Hughes et al., 2015).

Discussion point

- Identify two assets/systems where liquefaction legacy effects matter most (e.g., gravity sewer gradients, stopbank levels, road basecourse performance). Discuss what monitoring metric you would track to separate (a) ongoing consolidation/creep from (b) future event susceptibility.

Synthesis: Avonside as a practitioner case study for modern + paleo liquefaction

Avonside demonstrates three practitioner-relevant principles:

3. **Recurrent liquefaction is predictable in space** when geomorphic setting and conduit reactivation dominate; this has major implications for land performance classification (Quigley et al., 2013; Townsend et al., 2016).
4. **Paleoliquefaction evidence can occur where modern liquefaction is concentrated**, but preservation is selective and must be evaluated with strict stratigraphic and taphonomic criteria (Bastin et al., 2015; Villamor et al., 2016).
5. Liquefaction can produce **system-scale, long-lived consequences** (subsidence and flood hazard amplification) that should be treated as part of the hazard "portfolio," not as a separate post-event recovery issue (Hughes et al., 2015).

REFERENCES

Bastin, S. H., Quigley, M. C., Bassett, K., & Green, R. A. (2015). Paleoliquefaction in Christchurch, New Zealand. Geological Society of America Bulletin. https://doi.org/10.1130/B31174.1

Cubrinovski, M., & Green, R. A. (Eds.). (2010). Geotechnical reconnaissance of the 2010 Darfield (Canterbury) earthquake. Bulletin of the New Zealand Society for Earthquake Engineering, 43(4), 243–320.

Hughes, M. W., Quigley, M. C., van Ballegooy, S., Deam, B. L., Bradley, B. A., & Rhoades, D. A. (2015). The sinking city: Earthquakes increase flood hazard in Christchurch, New Zealand. GSA Today, 25(3), 4–10. https://doi.org/10.1130/GSATG221A.1

Quigley, M. C., Bastin, S., & Bradley, B. A. (2013). Recurrent liquefaction in Christchurch, New Zealand, during the Canterbury earthquake sequence. Geology, 41(4), 419–422. https://doi.org/10.1130/G33944.1

Reid, C. M., Thompson, N. K., Irvine, J. R. M., & Laird, T. E. (2012). Sand volcanoes in the Avon–Heathcote Estuary produced by the 2010–2011 Christchurch earthquakes: Implications for geological preservation and expression. New Zealand Journal of Geology and Geophysics, 55(3), 249–254. https://doi.org/10.1080/00288306.2012.674051

Townsend, D., Lee, J. M., Strong, D. T., Jongens, R., Smith Lyttle, B., Ashraf, S., Rosser, B., Perrin, N., Lyttle, K., Cubrinovski, M., & et al. (2016). Mapping surface liquefaction caused by the September 2010 and February 2011 Canterbury earthquakes: A digital dataset. New Zealand Journal of Geology and Geophysics. https://doi.org/10.1080/00288306.2016.1182929

Villamor, P., Almond, P., Tuttle, M. P., Giona-Bucci, M., Langridge, R. M., Clark, K., Ries, W., Bastin, S. H., Eger, A., Vandergoes, M., Quigley, M. C., Barker, P., Martin, F., & Howarth, J. (2016). Liquefaction features produced by the 2010–2011 Canterbury earthquake sequence in southwest Christchurch, New Zealand, and preliminary assessment of paleoliquefaction features. Bulletin of the Seismological Society of America, 106(4), 1747–1771. https://doi.org/10.1785/0120150223

Figure 2. A–F: Field photographs (looking southwest) of sand blows at study site following the (A) Darfield M_L 7.1 earthquake, (B) 22 February 2011 M_L 6.3, 5.8, and 5.9 earthquakes, (C) 16 April 2011 M_L 5.5 earthquake, (D) 13 June 2011-a M_L 5.6 earthquake, (E) 13 June 2011-b M_L 6.4 earthquake, and (F) 23 December 2011 M_L 5.8 and 6.0 earthquakes. All photos were taken from same location within 3 h of last inducing earthquake. G: Distinct liquefaction ejecta units in sand blow stratigraphy. Arrows and nails denote silt drapes. Cross-bedding as sketched. Location of photographed portion of trench location shown in F. H: Microrill development in silt drape at edge of a sand blow. I: Post-depositional erosion of sand blow and silt drape to form parabolic microdunes and ripples only 2 mo after formation.

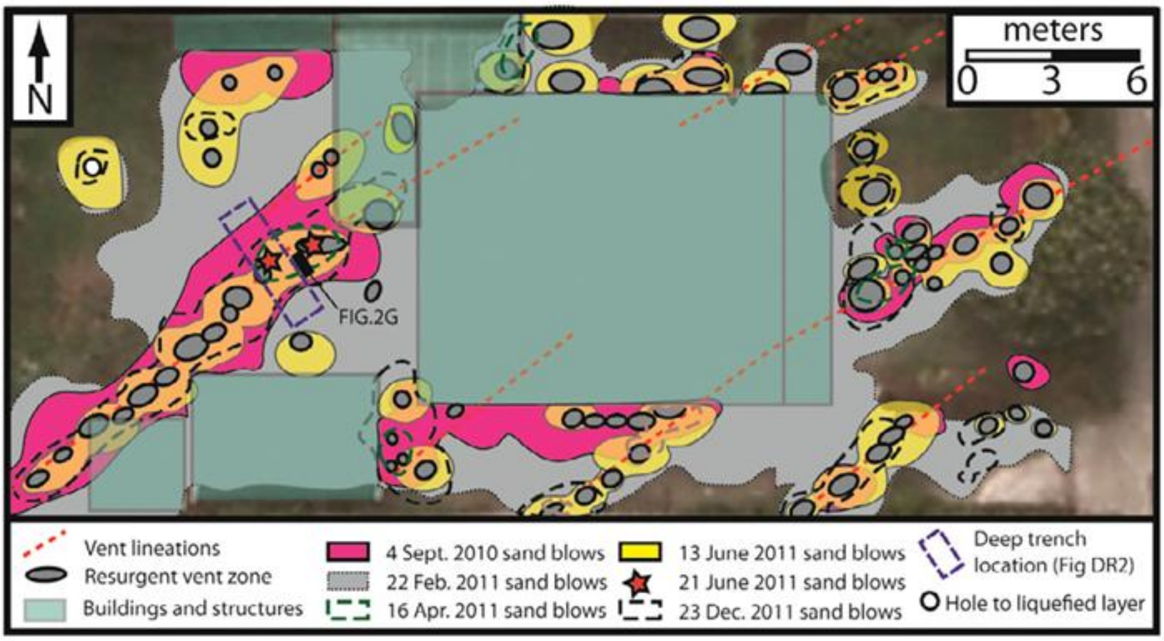

Figure 3. Detailed map of sand blows and source vents at study site for liquefaction-inducing Canterbury earthquake sequence (CES) events. Mapped extents reflect cumulative sediment deposition from multiple events for the 22 February, 13 June, and 23 December 2011 earthquakes. Areal extents in square meters and as a percent of total study site area are Darfield (65 m^2; 12%), 22 February (344 m^2; 64%), 16 April (6 m^2; 1%),) 13 June (78 m^2; 14%), 21 June (1 m^2; <1%), and 23 December (43 m^2; 8%). Fig. DR2 is Figure DR2 in the Data Repository (see footnote 1).

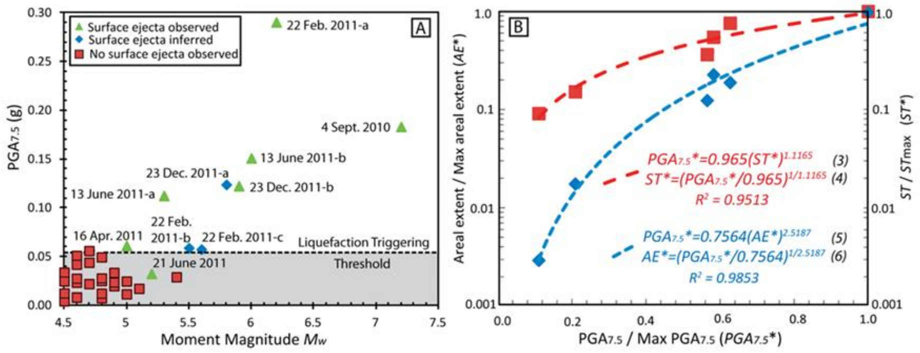

Figure 4. A: Peak ground acceleration normalized to M_w 7.5 earthquake ($PGA_{7.5}$) versus M_w and relationship to approximate liquefaction-triggering threshold for selected M_w ≥4.5 earthquakes. Liquefaction-triggering threshold of 0.056 g $PGA_{7.5}$ is shown. B: Sand blow areal extent (*AE*), maximum stratigraphic thickness (*ST*), and $PGA_{7.5}$ normalized to 22 February 2011 earthquake maxima (*AE, *ST**, $PGA_{7.5}$*), and corresponding power-law Equations 3–6.**

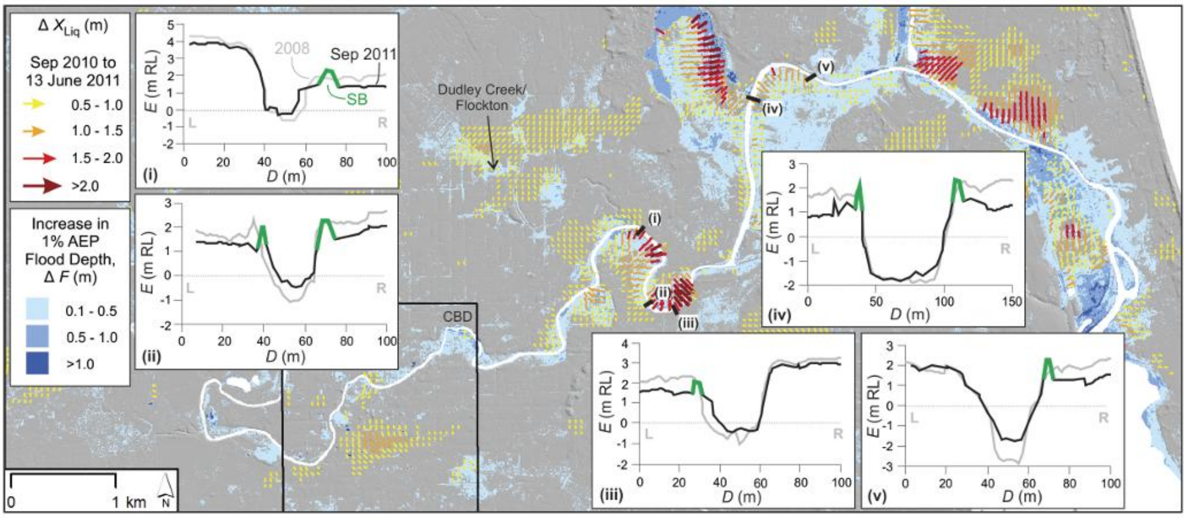

Figure 3. Main map: Cumulative horizontal movements (ΔX_{Liq}) in Christchurch in the vicinity of the Avon River from Sept. 2010 to 13 June 2011, derived from LiDAR offset analysis (Beavan et al., 2012a). Also shown: Increased 1-in-100-year storm event (1% Annual Exceedence Probability [AEP]) flood depths (ΔF) due to subsidence caused by the Canterbury Earthquake Sequence using current sea level, rainfall, and urban extent. The Christchurch Central Business District (CBD) is shown, as is the Dudley Creek/Flockton area where recent flooding of residential properties has been problematic. Inset panels: Floodplain and river cross sections (i–v) obtained from field survey and LiDAR analyses, with elevation (*E*) changes shown as relative level in meters (m RL) from 2008 (solid gray lines) to Sept. 2011 (black lines). Transect distance (*D*) is in meters (m). The locations of stopbanks (SB) constructed after the 22 Feb. 2011 Christchurch earthquake are shown in green.

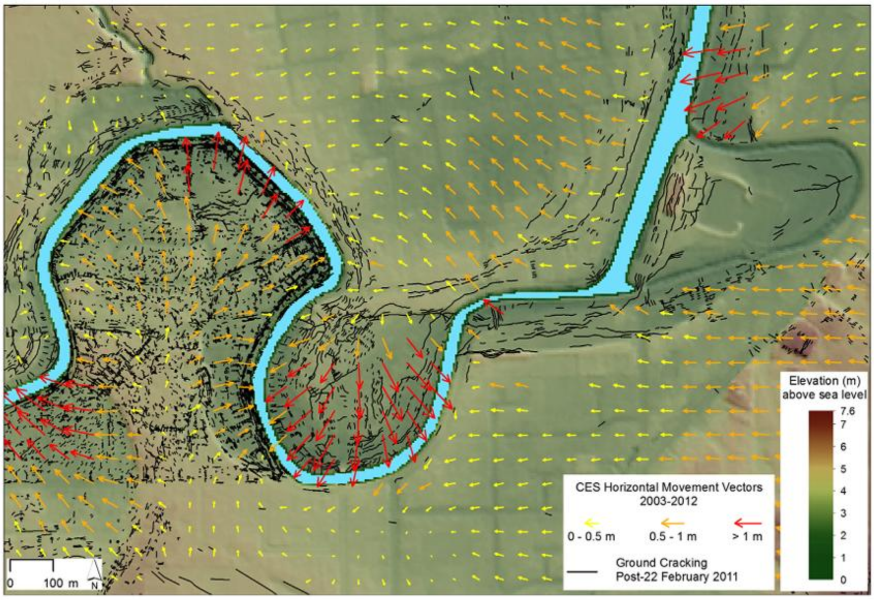

Fig. 13. Liquefaction and lateral spreading effects around a section of the Avon River in eastern Christchurch. Horizontal movement vectors record cumulative liquefaction related displacements from pre-CES to post M_w 5.9 December 2011 earthquake (i.e. the horizontal tectonic movement component as estimated by Beavan et al., 2012, have been removed from the vectors). Vectors are scaled for displacement and show spreading towards most proximal free faces (river channel) and / or lowest topography (e.g., western bank of the anthropogenically straightened river section on the eastern part of the image). Horizontal displacements in inner river meanders were particularly large, commonly exceeding 1 m, whereas outer, higher elevation river bends did not incur as severe ground cracking or displacements. Fissure mapping from Bastin et al. (2013) and Hughes et al. (2015) following the M_w 6.2 Christchurch earthquake reveal general increases in crack density and length with decreased distance to free faces; cracks will repeatedly reactivated throughout the CES however the effects in this area were most severe M_w 6.2 Christchurch earthquake (Quigley et al., 2013).

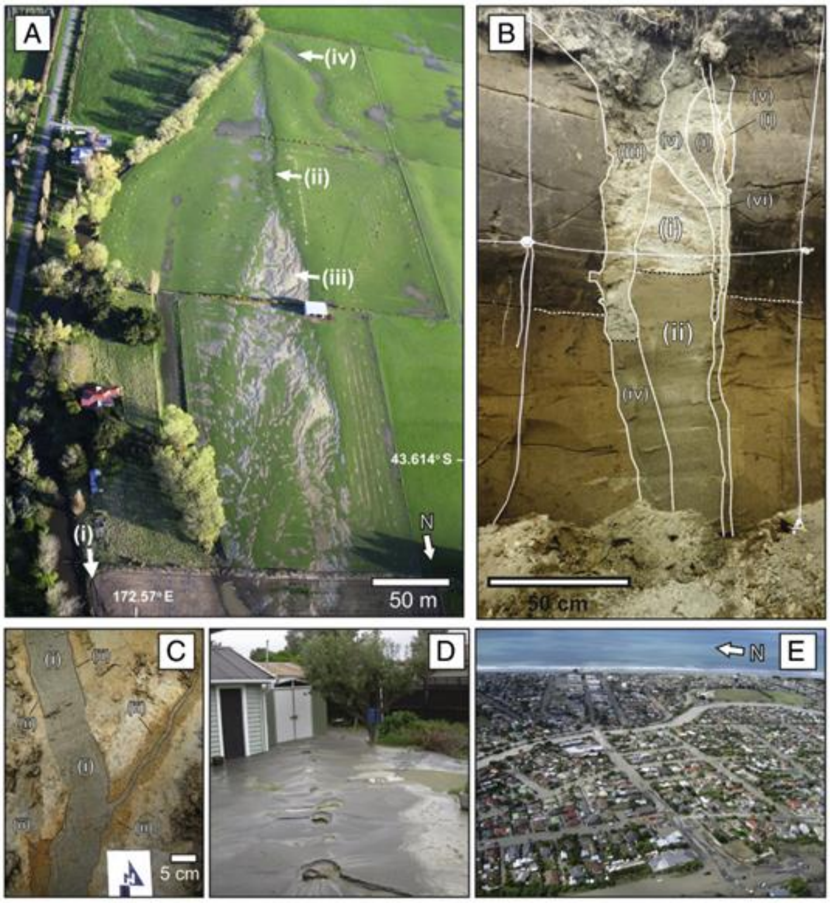

Fig. 9. Selected field photographs of liquefaction-induced environmental impacts. (A) Oblique aerial photograph of liquefaction features, lateral spreading, and flooding in southwest Christchurch west of Tai Tapu Stream three days after the Darfield earthquake. (i–ii) Lateral spreading features with large (>20–30 cm) fissure widths and no surface ejecta, typically within 5 m of modern (i) or (ii) paleochannel edges. (iii) Extensive sand blow fields fed by linear en-echelon feeder dike arrays perpendicular to lateral spreading direction and influenced by elevation and paleochannel geometries. (iv) Filling of paleochannels with flood waters and suspended liquefaction ejecta. (B) Multiple generations of CES liquefaction feeder dikes filling lateral spreading fissures in eastern Christchurch. Sequentially ordered from (i) oldest to (vi) youngest feeder dike generations. Dashed black lines show position of intradike stalling levels defined by fining-upward concentration of silts; interpreted to represent dike reactivation and dike sediment remobilization up to dashed line following initial dike formation (suggesting 6 distinct feeder dike generations), or settling of fines concurrent with dike formation (4 distinct generations). Dashed white lines show vertical displacement of soil profile across lateral spreading fissure, with downthrown side toward the Avon River in this instance. The number of 4 to 6 distinct dike generations is consistent with observation of 6 distinct earthquakes with PGA ≥ 0.2 g ($PGA_{7.5}$ ≥ 0.11 g) recorded for the study area (Quigley et al., 2013); favoured interpretation is (i,ii) Darfield earthquake; (iii,iv) Februrary earthquake(s); (v) June earthquake(s), (vi) December earthquake(s). (C) (i) Composite CES feeder dikes (≥3 generations identified by cross-cutting relationships defined by internal silt linings, varying compositions and grain sizes) that cross-cut and reactivate (ii) paleo-feeder dikes with increased oxidation, mottling, and bioturbated dike edges (modified from Bastin et al., 2015). (D) Large (≥2–3 m diameter) sand blows formed during the Mw 6.2 Christchurch earthquake. Sand blows formed at this site in at least 7 distinct earthquakes. Feeder dike reactivation resulted in venting at the same location in successive events (Quigley et al., 2013). (E) Liquefaction and subsidence-induced flooding in eastern Christchurch 1 day after the M_w 6.2 Christchurch earthquake. Flood water colouration due to presence of suspended liquefaction ejecta. More than 0.4 m of tectonic and vertical subsidence has resulted in elevations.

PLATINUM SPONSOR

Earth Sciences New Zealand

GOLD SPONSORS

Environment Canterbury Regional Council
Kaunihera Taiao ki Waitaha

UC UNIVERSITY OF CANTERBURY
Te Whare Wānanga o Waitaha
CHRISTCHURCH NEW ZEALAND

SILVER SPONSORS

luminescence dating. VICUS

Natural Hazards Commission
Toka Tū Ake

BRONZE SPONSOR + YOUNG GEOMORPHOLOGY TRAINING PROGRAM SPONSORS

ZEALANDIA Consulting

EGU European Geosciences Union

BSG British Society for Geomorphology

11TH IAG INTERNATIONAL CONFERENCE ON GEOMORPHOLOGY